Department of
OCEANOGRAPHY

OSU

SCHOOL OF SCIENCE

OREGON STATE UNIVERSITY

1970 Totem Wind and Current Data
by
Members of the THEMIS Group
Compiled by Noel B. Plutchak

Office of Naval Research
Contract N00014-68-A-0148
Project NR 083-102

Data Report 52 Reference 72-13
May 1972

School of Oceanography
Oregon State University
Corvallis, Oregon 97331

1970 TOTEM WIND AND CURRENT DATA

By Members of the THEMIS Group
Compiled by Noel B. Plutchak

Data Report No. 52

Office of Naval Research
Contract N 00014-68-A-0148
Project NR 083-230

Distribution of this document is unlimited

Reference 72-13
May 1972

John V. Byrne
Acting Dean

ABSTRACT

First-order analyses of wind and current time series obtained from a Totem buoy off the Oregon coast during 1970 are presented. In addition, winds at Totem are compared with winds recorded simultaneously at Newport, Oregon.

ACKNOWLEDGEMENTS

This research was supported by the Office of Naval Research contract N00014-68-A-0148 under project NR 083-230, and Sea Grant project GH-97. The assistance of William Gilbert and Michael Gaughan is gratefully acknowledged.

TABLE OF CONTENTS

FIGURES

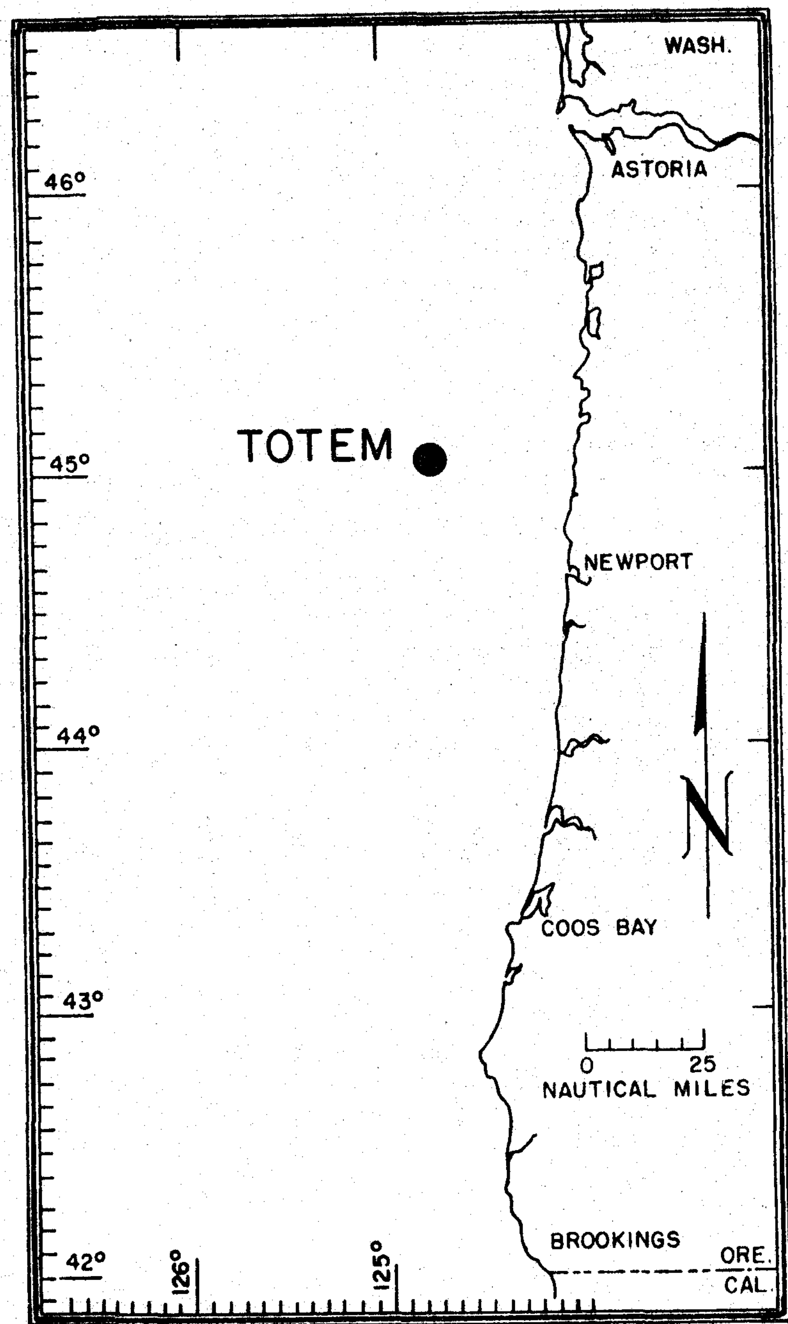

Figure 1. TOTEM Location map.

INTRODUCTION

The aim of the TOTEM project is real-time acquisition and analysis of air-sea data from a stable buoy.

The Totem buoy structural design and deployment technique evolved during the three years preceding 1970. The resultant structure is a quasi-cylindrical spar buoy 180 ft. long and 6 ft. in diameter. The buoy is towed to station horizontally, erected by flooding ballast tanks, and moored by a two-point system utilizing spring buoys. Freeboard of one-sixth the buoy's length provides a stable platform with adequate room for instruments, power supplies, navigational aids and data acquisition and telemetry equipment. Details of Totem structure, mooring and deployment are the subjects of separate reports.[1]

A system of data processing and analysis techniques has been developed concurrently with the buoy system. Winds and currents were recorded on strip charts during 1970 to test the data processing and analysis system prior to initiating a telemetry link between the buoy and shore-based computer. Analyses of these data are presented in this report. Analyses of real-time, telemetered data are described in a report now in preparation.

The Totem I buoy was located at 44°59.6'N., 124°44.7'W., a position of about 35 miles northwest of Newport, Oregon (Fig. 1). From 16 May to 20 September 1970 the record of winds is continuous, except for a break between 6 June and 17 July. The record of currents extends from 5 August - 14 August, 1970. The winds and currents are described through:

Gross Statistics (means, variances, etc.);
Histograms (u-, v-components and speed);
Scattergrams (u vs. v and speed vs. direction);
Progressive Vector Diagrams (a quasi-trajectory representation);
Time Series Plots (u, v and speed vs. time); and
Spectral Analyses (spectral density and correlation).

A comparison is made of winds measured at Totem and Newport, and the results of an investigation of the diurnal periodicity of winds at Totem are given.

The instruments and techniques of data processing and analyses that were employed are briefly described. The digitized, edited data is available on magnetic tape.[2]

---

[1]This buoy is described in the following two reports:
(a) Dominguez, Nath, et al., 1969. Analysis of a two-point mooring for a spar buoy. Dept. Oceanography, Ref. 69-34, Oregon State Univ.
(b) Young and Neshyba, 1970. Engineering design and usage of the TOTEM buoy. Dept. Oceanography, Ref. 70-19, Oregon State Univ.

[2] (File MT 9085)

INSTRUMENTATION

Wind speed and direction at Totem are sensed by a Skyvane anemometer (Model 101-DC) and recorded as two continuous traces by a Rustrak recorder (Model 388) at a rate of one-half inch per hour. The anemometer is mounted at the top of a tower which extends 3 m above the Totem structure and 10 m above sea level.

Currents are measured with a BENDIX-Marine Advisers' Ducted Meter (Model Q-15) extended 20 feet from Totem at 7 m depth, and recorded on strip chart as speed and direction on the second channel of the wind recorder.

DATA PROCESSING

The chart records of speed and direction were digitized to form data series at 10-min intervals. The wind record of 16 May to 6 June was manually digitized at the 10-min intervals. All other data were mechanically digitized at 1.2 min intervals by the Calma Digitizer located at the O.S.U. Computer Center, and were then block-averaged[3] to form ten-min interval series. The digitization was inspected for errors by superimposing chart records on plots[4] of the digitized series of identical scales. Few errors were detected, and these were corrected by interpolation (or redigitized). Wind and current velocity component series [v - toward the north (true), u - toward the east] were formed[5] from the edited speed and direction series.

ANALYSES OF TOTEM WINDS

A. Gross Statistics

The following statistical measures were computed[6] from the ten-min interval series for each month (May through September), where C (I) = 1, 2, . . ., N represents the u-component, v-component or speed series:

---

[3]Themis Program: *TOTENAVG

[4]Themis Program: *FINAL WIND and FINAL CUR

[5]Themis Program: *COMPUV

[6]Themis Program: *GROSS

MEAN = mean = $\overline{C} = 1/N \sum_{I=1}^{N} C(I)$

VAR = variance = $\sigma^2 = 1/N \sum_{I=1}^{N} [C'(I)]^2$

STD = standard deviation = σ = SQRT $[\sigma^2]$

STE = standard error = SQRT $[\sigma^2/N]$

MDEV = mean magnitude of deviations = $\overline{|C'|} = 1/N \sum_{I=1}^{N} |C'(I)|$

where $C'(I) = C(I) - \overline{C}$

CORNU = Cornu ratio = $\sigma^2 / \overline{(|C'|)}$ **2

SKEW = skewness = $\{1/N \sum_{I=1}^{N} [C'(I)]^3\}/\sigma^3$

KURT = kurtosis = $\{1/N \sum_{I=1}^{N} [C'(I)]^4\}/\sigma^4$

With $C_x(I)$ representing the u-component series and $C_y(I)$ the v-component series, the following were computed:

COV = covariance = $1/N \sum_{I=1}^{N} [C_x'(I) * C_y'(I)]$

COR = correlation coefficient = COV/ $(\sigma_x * \sigma_y)$

VARCO = variance of correlation = $\sigma_{co}^2 = 1/N \sum_{I=1}^{N} [(C_x'(I) * C_y'(I))**2]$

STDCO = standard deviation of covariance = σ_{co} = SQRT (σ_{co}^2)

STECO = standard error of covariance = SQRT $[\sigma_{co}^2/N]$

RI = isotropy ratio = SQRT $[\sigma_x^2/\sigma_y^2]$

VMS = vector magnitude series = $|\hat{C}(I)|$ = SQRT$[C_x(I)$ **2 + $C_y(I)$ **2]

SM = scalar mean (mean vector magnitude) = $\overline{|\hat{C}|} = 1/N \sum_{I=1}^{N} |\hat{C}(I)|$

VM = vector mean = $|\overline{\hat{C}}|$ = SQRT $[\overline{C}_x$**2 + $\overline{C}_y$ ** 2]

VARV = vector variance = $\sigma_v^2 = [\sigma_x^2 + \sigma_y^2]/2.0$

STDV = vector standard deviation = σ_v = SQRT $[\sigma_v^2]$

STEV = vector standard error = SQRT $[\sigma_v^2/N]$

IFX = intensity of x-directed fluctuations = $\sigma_x/(\overline{|\hat{C}|})$

IFY = intensity of y-directed fluctuations - $\sigma_y/(\overline{|\hat{C}|})$

These computations are listed in Tables I - VI.

Normality of the u-component, v-component and speed distributions of each month were tested[7] using the Cornu ratio and skewness. The results of these tests for 90, 95 and 99 percent confidence levels are listed in Tables I - VI by P (Pass) and F (Fail). A variable is considered not to be normally distributed at some level of confidence if either or both the Cornu and skewness tests fail.

B. Histograms

Histograms of the 16 May through 6 June winds are shown in Fig. 2; these illustrate the marked nonstationarity during this period. Frequency distributions of wind speeds and u- and v-components during July, August and September are shown in the histograms[8] of Fig. 3. Also included in this figure are histograms of the current measured at Totem at a depth of 7 m during August.

---

[7]See: O'Brien, J.J. and J.F. Griffiths, 1967. Choosing a test of normality for small samples. Archiv. fur Meteorologie, Geophysik and Bioklimatologie, Ser. A, 16 (213), 267-272.

or

H. Crew and Gudrun Bodvarsson, 1971. Testing data for normality (informal memo, Department of Oceanography, OSU)

[8]Themis Program: #HISTL

DATA OF: May Totem Wind (N = 2688)

TABLE I

Statistic	U	V	Speed
	Data Series		
MEAN	.0221	-5.3765	6.9588
VAR	6.1352	30.2360	16.8538
STD	2.4769	5.4987	4.1053
STE	.0478	.1061	.0792
MDEV	1.5049	4.6806	3.5246
CORNU	2.7092	1.3801	1.3567
DC	72.4721	-12.1401	-13.6290
SKEW	.2012	.3047	-0.0751
KURT	5.4389	2.1887	1.8874
COV	-4.1729		
COR	-0.3064		
VARCO	171.9582		
STDCO	13.1133		
STECO	.2529		
RI	.4505		
SM	6.9588		
VM	5.3766		
VARV	18.1856		
STDV	4.2645		
STEV	.0823		
IFX	.3559		
IFY	.7902		
DVR	.7726		
Normality tests			
Skewness (90%)	F	F	P
Skewness (95%)	F	F	P
Cornu (90%)	F	F	F
Cornu (95%)	F	F	F
Skewness (99%)	F	F	P
Cornu (99%)	F	F	F

DATA OF: Totem Wind 1450 July 17 to 2400, July 31 (N = 2077)

TABLE II

Statistic	Data Series U	Data Series V	Data Series Speed
MEAN	-2.1277	-5.3989	7.9639
VAR	17.1339	31.3138	18.6991
STD	4.1393	5.5959	4.3242
STE	.0908	.1228	.0949
MDEV	3.3611	4.6269	3.6608
CORNU	1.5167	1.4627	1.3953
DC	-3.4472	-6.8823	-11.1711
SKEW	.6269	.4798	.0203
KURT	2.7786	2.4992	1.9696
COV	20.4486		
COR	.8828		
VARCO	1182.3916		
STDCO	34.3359		
STECO	.7545		
RI	.7397		
SM	7.9639		
VM	5.8030		
VARV	24.2239		
STDV	4.9218		
STEV	.1080		
IFX	.5198		
IFY	.7027		
DVR	.7287		
Normality tests			
Skewness (90%)	F	F	P
Skewness (95%)	F	F	P
Cornu (90%)	F	F	F
Cornu (95%)	F	F	F
Skewness (99%)	F	F	P
Cornu (99%)	P	F	F

DATA OF: Aug. 1 - 0151 - Sept. 1 Totem Wind (N = 4463)

TABLE III

Statistic	Data Series U	V	Speed
MEAN	-2.0438	-5.6291	8.7398
VAR	12.4238	50.1758	22.0793
STD	3.5247	7.0835	4.6989
STE	.0528	.1060	.0703
MDEV	2.9423	5.9272	3.9210
CORNU	1.4351	1.4282	1.4361
DC	-8.6407	-9.0771	-8.5759
SKEW	.5250	.5197	-0.0278
KURT	2.3649	2.4234	2.1687
COV	21.6950		
COR	.8689		
VARCO	1124.2150		
STDCO	33.5293		
STECO	.5019		
RI	.4976		
SM	8.7398		
VM	5.9886		
VARV	31.2998		
STDV	5.5946		
STEV	.0837		
IFX	.4033		
IFY	.8105		
DVR	.6852		
Normality tests			
Skewness (90%)	F	F	P
Skewness (95%)	F	F	P
Cornu (90%)	F	F	F
Cornu (95%)	F	F	F
Skewness (99%)	F	F	P
Cornu (99%)	F	F	F

DATA OF: 1643 Sept 2 - 0900 Sept. 15 Totem Wind (N = 1825)

TABLE IV

Statistic	Data Series U	V	Speed
MEAN	-0.6795	-5.0816	8.2039
VAR	26.1095	39.2279	24.3179
STD	5.1097	6.2632	4.9313
STE	.1196	.1466	.1154
MDEV	4.1315	5.1327	4.1799
CORNU	1.5296	1.4890	1.3919
DC	-2.6239	-5.2053	-11.3902
SKEW	.2355	.1239	.1877
KURT	2.6377	2.4539	2.0060
COV	23.6623		
COR	.7394		
VARCO	1560.0950		
STDCO	39.4980		
STECO	.9246		
RI	.8158		
SM	8.2039		
VM	5.1269		
VARV	32.6687		
STDV	5.7157		
STEV	.1338		
IFX	.6228		
IFY	.7634		
DVR	.6249		
Normality tests			
Skewness (90%)	F	F	F
Skewness (95%)	F	F	F
Cornu (90%)	F	F	F
Cornu (95%)	P	F	F
Skewness (99%)	F	P	F
Cornu (99%)	P	F	F

DATA OF: 5 - 14 Aug. Wind (N = 1328)

TABLE V

Statistic	U	V	Speed
	Data Series		
MEAN	-2.3181	-6.4767	10.2448
VAR	17.3734	62.4386	22.1763
STD	4.1681	7.9018	4.7092
STE	.1144	.2168	.1292
MDEV	3.5833	6.7973	4.1208
CORNU	1.3530	1.3514	1.3060
DC	-13.8633	-13.9684	-16.8605
SKEW	.5438	.5718	-0.0646
KURT	2.0705	2.0376	1.7942
COV	30.1332		
COR	.9149		
VARCO	1785.7473		
STDCO	42.2581		
STECO	1.1596		
RI	.5275		
SM	10.2448		
VM	6.8790		
VARV	39.9060		
STDV	6.3171		
STEV	.1733		
IFX	.4069		
IFY	.7713		
DVR	.6715		
Normality tests			
Skewness (90%)	F	F	P
Skewness (95%)	F	F	P
Cornu (90%)	F	F	F
Cornu (95%)	F	F	F
Skewness (99%)	F	F	P
Cornu (99%)	F	F	F

DATA OF: 1132 Aug. 4 - 1627 Aug. 14 Current (N = 1328)

TABLE VI

Statistic	Data Series: U	V	Speed
MEAN	-0.0077	-0.1382	.1793
VAR	.0101	.0093	.0065
STD	.1007	.0965	.0804
STE	.0028	.0026	.0022
MDEV	.0788	.0767	.0645
CORNU	1.6347	1.5825	1.5534
DC	4.0686	.7456	-1.1068
SKEW	.1045	.2272	.2951
KURT	3.0144	2.8974	3.0391
COV	.0020		
COR	.2063		
VARCO	.0001		
STDCO	.0114		
STECO	.0003		
RI	1.0435		
SM	.1793		
VM	.1384		
VARV	.0097		
STDV	.0986		
STEV	.0027		
IFX	.5616		
IFY	.5382		
DVR	.7718		
Normality tests			
Skewness (90%)	P	F	F
Skewness (95%)	P	F	F
Cornu (90%)	F	P	P
Cornu (95%)	F	P	P
Skewness (99%)	P	F	F
Cornu (99%)	F	P	P

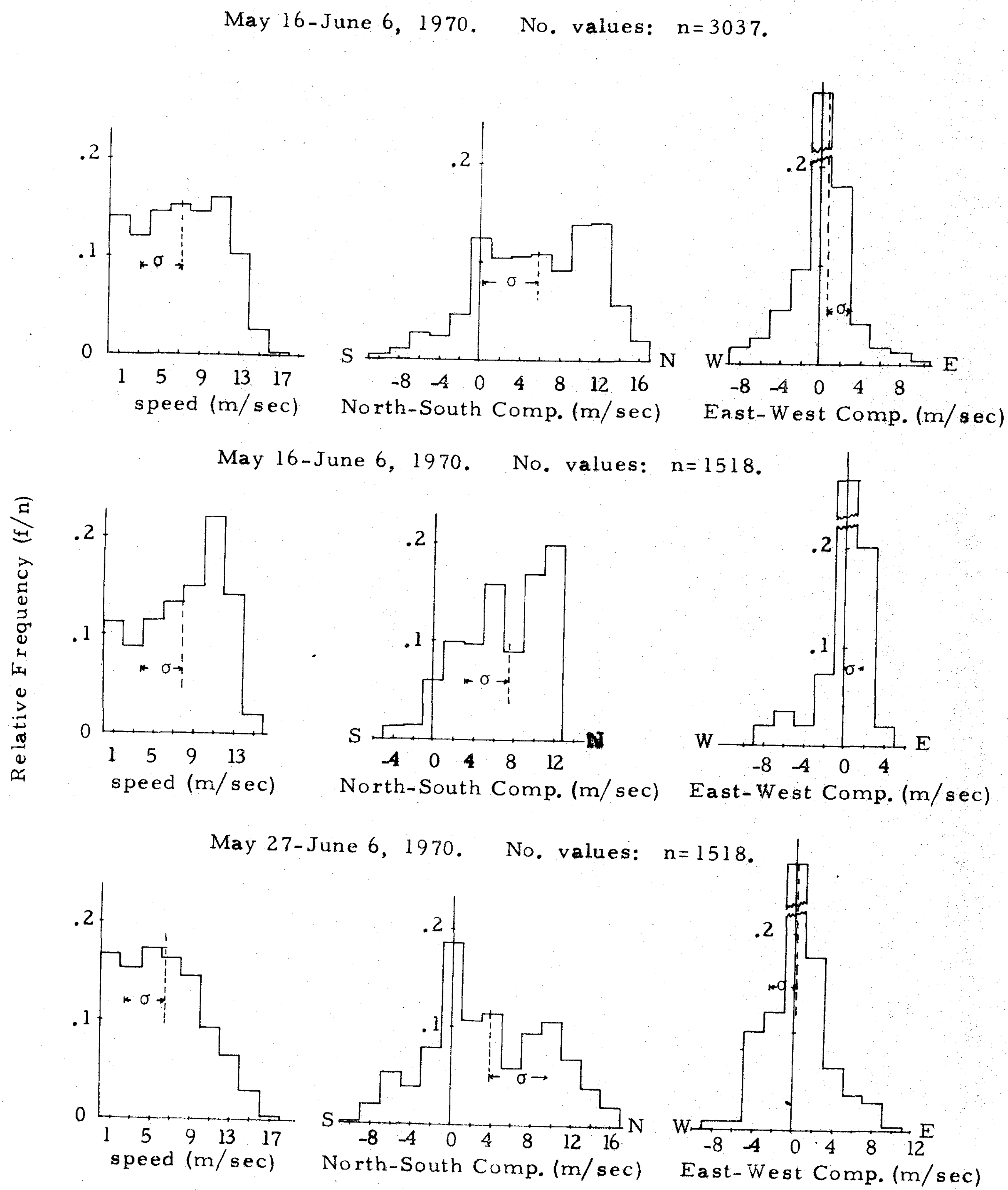

Fig. 2 . Histograms of Totem Wind Speeds and Velocity Components

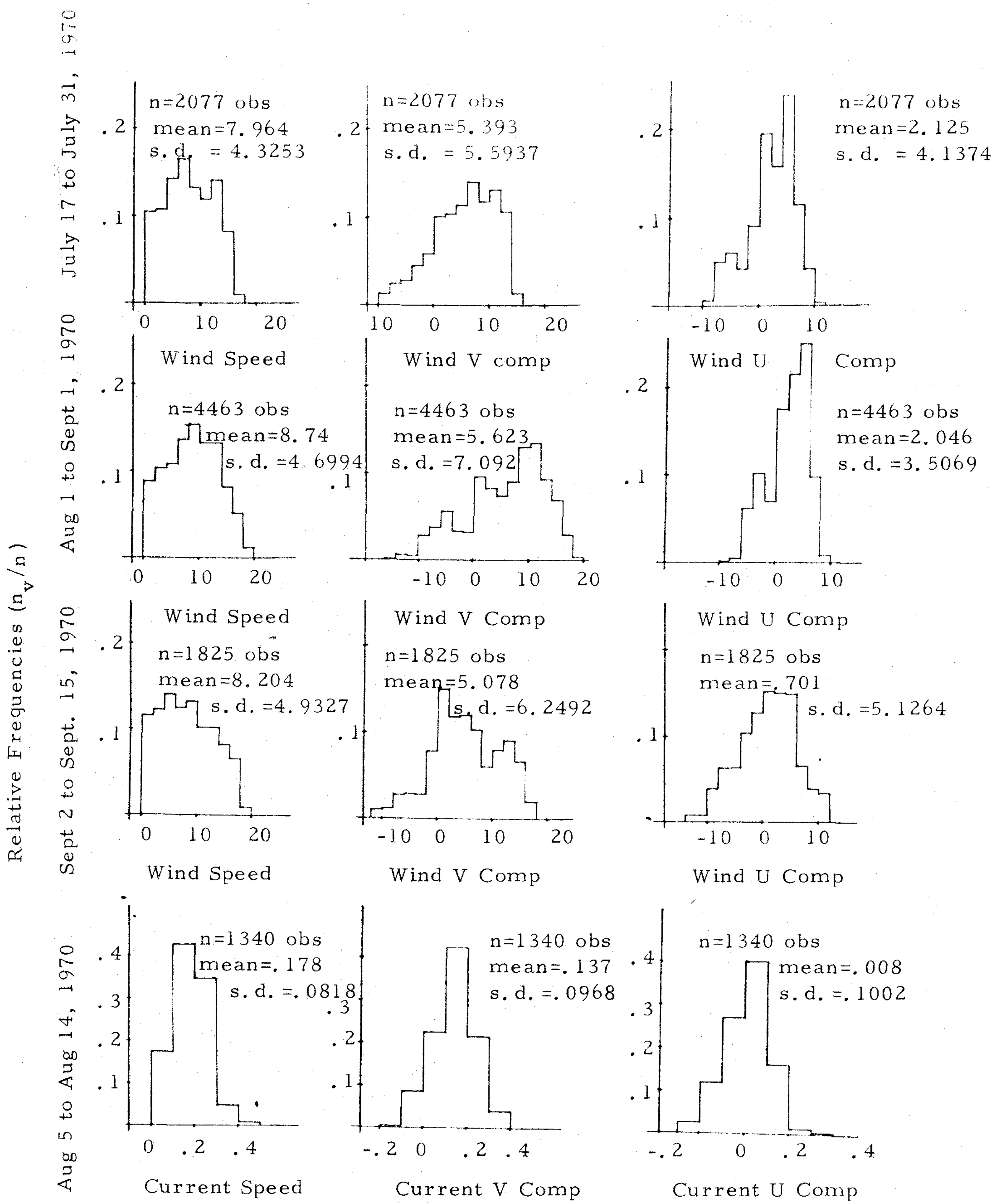

Figure 3. Histograms of Totem 1970 wind and current speeds, U and V components (in meters/sec)

C. Scattergrams

Two-dimensional frequency distributions[9] (or numerical scattergrams) of wind and current speed, direction and velocity components are shown in Figs. 4 through 11. In these scattergrams, speed is in meter/sec and direction is measured positive clockwise from true north in radians.

The scattergrams of wind speed vs. wind direction indicate a biomodiality of wind direction which is especially pronounced in some speed ranges.

The intensity of wind direction bimodality, as well as the magnitude of wind speed, increases from May through August (Figures 4a, 5a, and 6a). At higher wind speeds the primary direction of the wind is sharply limited; for example, at wind speeds greater than 6.0 m/sec during August, there were 2094 occurrences in the 30 degree direction interval 3.14-3.66 radians, and only 8 occurrences in the neighboring 30 degree interval 2.62-3.14 radians.

The scattergrams of u-v wind components also indicate the 180° bimodality of wind direction. These "wind roses" are approximately elliptical with the coordinate origin located close to the major axis. In May (Fig. 4b) the major axis was directed N-S, while during July, August and September (Figs. 5b, 6b and 7b) it was directed SW-NE. The intensity of bimodality was least during September, due to smaller ellipticity of the distribution and greater displacement of the coordinate origin from the major axis.

Scattergrams of the currents (Figs. 9a, b) indicate generally southerly drifts with no evidence of bimodality. The "current rose" of Fig. 9c shows that the mean current speed was largely independent of direction, except in the NW quadrant where it was significantly lower. No obvious functional relations between wind and current speeds and directions are evident in Figs. 11 a-d. Fig. 11c shows that the wind and current were often in the same direction (southward); in these cases the wind increased the (southward) momentum of the water. Although winds and currents were most often southward, and their speeds were greatest in this direction, Figure 11b shows that the mean wind speed was greatest when the currents were northward. A possible explanation is that the high winds of the storm created a rotary inertial motion of greater speed than the general southward drift; the currents would then be northward at times during the storm, and rarely (if at all) northward during periods of lower wind speeds.

---

[9]Themis Program: #SCATTE

INTERVAL NUMBER	SPEED MY LOWER	SPEED MY UPPER	NUMBER OF OBS	DIR MAY LOWER	DIR MAY UPPER	NUMBER OF OBS
1	0	2.000	362	0	.524	65
2	2.000	4.000	332	.524	1.047	8
3	4.000	6.000	393	1.047	1.571	8
4	6.000	8.000	432	1.571	2.094	26
5	8.000	10.000	381	2.094	2.618	153
6	10.000	12.000	446	2.618	3.142	441
7	12.000	14.000	289	3.142	3.665	1537
8	14.000	16.000	33	3.665	4.189	68
9	16.000	18.000	0	4.189	4.712	55
10	18.000	20.000	0	4.712	5.236	120
11				5.236	5.759	128
12				5.759	6.283	79

SCATTER DIAGRAM

SPEED

10.	0.	0.	0.	0.	0.	0.	0.	0.	0.	0.	0.	0.
9.	0.	0.	0.	0.	0.	0.	0.	0.	0.	0.	0.	0.
8.	0.	0.	0.	0.	0.	1.	32.	0.	0.	0.	0.	0.
7.	0.	0.	0.	0.	3.	80.	206.	0.	0.	0.	0.	0.
6.	0.	0.	0.	0.	26.	110.	310.	0.	0.	0.	0.	0.
5.	7.	0.	0.	14.	60.	79.	188.	0.	9.	2.	16.	6.
4.	28.	0.	0.	12.	31.	94.	172.	6.	17.	42.	12.	18.
3.	10.	5.	5.	0.	7.	31.	169.	47.	16.	22.	44.	37.
2.	11.	0.	0.	0.	17.	38.	157.	15.	3.	36.	43.	12.
1.	9.	3.	3.	0.	9.	8.	303.	0.	10.	18.	13.	6.
	1	2	3	4	5	6	7	8	9	10	11	12

DIR

Fig. 4a Scattergram

Wind Speed/Direction May 1970

INTERVAL NUMBER	U COMPMY LOWER	U COMPMY UPPER	NUMBER OF OBS	V COMPMY LOWER	V COMPMY UPPER	NUMBER OF OBS
1	-15.000	-13.000	0	-15.000	-13.000	131
2	-13.000	-11.000	0	-13.000	-11.000	393
3	-11.000	-9.000	1	-11.000	-9.000	368
4	-9.000	-7.000	43	-9.000	-7.000	227
5	-7.000	-5.000	55	-7.000	-5.000	342
6	-5.000	-3.000	102	-5.000	-3.000	282
7	-3.000	-1.000	418	-3.000	-1.000	262
8	-1.000	1.000	1504	-1.000	1.000	351
9	1.000	3.000	275	1.000	3.000	142
10	3.000	5.000	170	3.000	5.000	77
11	5.000	7.000	77	5.000	7.000	81
12	7.000	9.000	43	7.000	9.000	31
13	9.000	11.000	0	9.000	11.000	1
14	11.000	13.000	0	11.000	13.000	0
15	13.000	15.000	0	13.000	15.000	0

SCATTER DIAGRAM

V COMP

V COMP	1	2	3	4	5	6	7	8	9	10	11	12	13	14	15
15.	0.	0.	0.	0.	0.	0.	0.	0.	0.	0.	0.	0.	0.	0.	0.
14.	0.	0.	0.	0.	0.	0.	0.	0.	0.	0.	0.	0.	0.	0.	0.
13.	0.	0.	0.	0.	0.	0.	0.	0.	1.	0.	0.	0.	0.	0.	0.
12.	0.	0.	0.	0.	0.	3.	4.	15.	9.	0.	0.	0.	0.	0.	0.
11.	0.	0.	0.	0.	15.	11.	16.	29.	4.	6.	0.	0.	0.	0.	0.
10.	0.	0.	0.	4.	9.	9.	35.	11.	9.	0.	0.	0.	0.	0.	0.
9.	0.	0.	0.	13.	15.	20.	56.	30.	2.	6.	0.	0.	0.	0.	0.
8.	0.	0.	1.	25.	16.	21.	27.	258.	0.	0.	3.	0.	0.	0.	0.
7.	0.	0.	0.	1.	0.	10.	16.	194.	25.	1.	3.	12.	0.	0.	0.
6.	0.	0.	0.	0.	0.	21.	87.	128.	25.	1.	12.	8.	0.	0.	0.
5.	0.	0.	0.	0.	0.	4.	48.	164.	61.	28.	31.	6.	0.	0.	0.
4.	0.	0.	0.	0.	0.	2.	36.	64.	18.	69.	26.	12.	0.	0.	0.
3.	0.	0.	0.	0.	0.	1.	68.	214.	43.	35.	2.	5.	0.	0.	0.
2.	0.	0.	0.	0.	0.	0.	13.	286.	70.	24.	0.	0.	0.	0.	0.
1.	0.	0.	0.	0.	0.	0.	12.	111.	8.	0.	0.	0.	0.	0.	0.

U COMP

Figure 4b. Scattergram
Wind u/v Components May 1970

INTERVAL NUMBER	SPEED JUL LOWER	SPEED JUL UPPER	NUMBER OF OBS	DIR JUL LOWER	DIR JUL UPPER	NUMBER OF OBS
1	0.000	2.000	218	0.000	0.523	10
2	2.000	4.000	224	0.523	1.047	176
3	4.000	6.000	293	1.047	1.570	126
4	6.000	8.000	340	1.570	2.094	48
5	8.000	10.000	273	2.094	2.618	44
6	10.000	12.000	247	2.618	3.141	127
7	12.000	14.000	291	3.141	3.664	1009
8	14.000	16.000	170	3.664	4.188	440
9	16.000	18.000	20	4.188	4.711	46
10	18.000	20.000	0	4.711	5.235	18
11				5.235	5.758	3
12				5.758	6.282	29

SCATTER DIAGRAM

SPEED

SPEED	1	2	3	4	5	6	7	8	9	10	11	12
10.	0.	0.	0.	0.	0.	0.	0.	0.	0.	0.	0.	0.
9.	0.	0.	0.	0.	0.	0.	7.	13.	0.	0.	0.	0.
8.	0.	0.	0.	0.	0.	0.	98.	72.	0.	0.	0.	0.
7.	0.	1.	0.	0.	0.	0.	190.	100.	0.	0.	0.	0.
6.	0.	51.	0.	0.	0.	0.	139.	57.	0.	0.	0.	0.
5.	0.	39.	10.	0.	0.	0.	147.	75.	2.	0.	0.	0.
4.	1.	33.	32.	0.	0.	11.	159.	90.	12.	0.	0.	2.
3.	2.	41.	56.	11.	10.	26.	124.	13.	1.	0.	0.	9.
2.	0.	8.	17.	12.	21.	57.	85.	11.	1.	3.	0.	9.
1.	7.	3.	11.	25.	13.	33.	60.	9.	30.	15.	3.	9.

DIR

7.0

<u>Fig. 5a</u> Scattergram

Wind Speed/Direction July 17 - 31, 1970.

INTERVAL NUMBER	U COMPJUL LOWER	U COMPJUL UPPER	NUMBER OF OBS	V COMPJUL LOWER	V COMPJUL UPPER	NUMBER OF OBS
1	-2Ø.ØØØ	-16.ØØØ	Ø	-2Ø.ØØØ	-16.ØØØ	3
2	-16.ØØØ	-12.ØØØ	Ø	-16.ØØØ	-12.ØØØ	247
3	-12.ØØØ	-8.ØØØ	94	-12.ØØØ	-8.ØØØ	518
4	-8.ØØØ	-4.ØØØ	736	-8.ØØØ	-4.ØØØ	527
5	-4.ØØØ	Ø.ØØØ	713	-4.ØØØ	Ø.ØØØ	415
6	Ø.ØØØ	4.ØØØ	288	Ø.ØØØ	4.ØØØ	229
7	4.ØØØ	8.ØØØ	231	4.ØØØ	8.ØØØ	1Ø8
8	8.ØØØ	12.ØØØ	14	8.ØØØ	12.ØØØ	29
9	12.ØØØ	16.ØØØ	Ø	12.ØØØ	16.ØØØ	Ø
1Ø	16.ØØØ	2Ø.ØØØ	Ø	16.ØØØ	2Ø.ØØØ	Ø

SCATTER DIAGRAM

V COMP

1Ø.	Ø.	Ø.	Ø.	Ø.	Ø.	Ø.	Ø.	Ø.	Ø.	Ø.
9.	Ø.	Ø.	Ø.	Ø.	Ø.	Ø.	Ø.	Ø.	Ø.	Ø.
8.	Ø.	Ø.	Ø.	Ø.	Ø.	Ø.	27.	2.	Ø.	Ø.
7.	Ø.	Ø.	Ø.	Ø.	11.	7.	83.	7.	Ø.	Ø.
6.	Ø.	Ø.	Ø.	Ø.	38.	78.	1Ø8.	5.	Ø.	Ø.
5.	Ø.	Ø.	1.	26.	2Ø7.	158.	13.	Ø.	Ø.	Ø.
4.	Ø.	Ø.	2.	137.	353.	35.	Ø.	Ø.	Ø.	Ø.
3.	Ø.	Ø.	44.	393.	81.	Ø.	Ø.	Ø.	Ø.	Ø.
2.	Ø.	Ø.	47.	18Ø.	2Ø.	Ø.	Ø.	Ø.	Ø.	Ø.
1.	Ø.	Ø.	Ø.	Ø.	3.	Ø.	Ø.	Ø.	Ø.	Ø.
	1	2	3	4	5	6	7	8	9	1Ø

U COMP

Fig. 5b Scattergram

Wind U/V Components July 17 - 31, 1970.

INTERVAL NUMBER	SPEED AU LOWER	SPEED AU UPPER	NUMBER OF OBS	DIR AUG LOWER	DIR AUG UPPER	NUMBER OF OBS
1	0	2.000	390	0	.524	380
2	2.000	4.000	460	.524	1.047	418
3	4.000	6.000	482	1.047	1.570	66
4	6.000	8.000	612	1.570	2.094	74
5	8.000	10.000	690	2.094	2.617	92
6	10.000	12.000	589	2.617	3.141	144
7	12.000	14.000	590	3.141	3.664	2497
8	14.000	16.000	364	3.664	4.188	675
9	16.000	18.000	231	4.188	4.711	54
10	18.000	20.000	54	4.711	5.235	19
11				5.235	5.758	14
12				5.758	6.282	29

SCATTER DIAGRAM

SPEED

SPEED	1	2	3	4	5	6	7	8	9	10	11	12
10	0	0	0	0	0	0	54	0	0	0	0	0
9	0	0	0	0	0	0	224	7	0	0	0	0
8	4	0	0	0	0	0	343	17	0	0	0	0
7	45	0	0	0	0	0	434	111	0	0	0	0
6	43	5	0	2	0	1	417	121	0	0	0	0
5	127	37	5	0	0	4	397	120	0	0	0	0
4	85	186	15	1	3	3	225	91	3	0	0	0
3	45	115	21	3	8	33	160	87	9	0	0	1
2	9	49	8	43	32	65	150	68	20	11	4	1
1	22	26	17	25	49	38	93	53	22	8	10	27

DIR

Fig. 6a Scattergram

Wind Speed/Direction 1 - 31 August 1970

INTERVAL NUMBER	U COMPAG LOWER	U COMPAG UPPER	NUMBER OF OBS	V COMPAG LOWER	V COMPAG UPPER	NUMBER OF OBS
1	-20.000	-16.000	0	-20.000	-16.000	143
2	-16.000	-12.000	0	-16.000	-12.000	721
3	-12.000	-8.000	41	-12.000	-8.000	1175
4	-8.000	-4.000	1560	-8.000	-4.000	733
5	-4.000	0	1626	-4.000	0	680
6	0	4.000	929	0	4.000	403
7	4.000	8.000	302	4.000	8.000	418
8	8.000	12.000	5	8.000	12.000	155
9	12.000	16.000	0	12.000	16.000	35
10	16.000	20.000	0	16.000	20.000	0

SCATTER DIAGRAM

V COMP

10.	0.	0.	0.	0.	0.	0.	0.	0.	0.	0.
9.	0.	0.	0.	0.	0.	31.	4.	0.	0.	0.
8.	0.	0.	0.	0.	0.	73.	82.	0.	0.	0.
7.	0.	0.	0.	0.	1.	279.	138.	0.	0.	0.
6.	0.	0.	0.	0.	47.	278.	75.	3.	0.	0.
5.	0.	0.	0.	33.	421.	221.	3.	2.	0.	0.
4.	0.	0.	2.	205.	484.	42.	0.	0.	0.	0.
3.	0.	0.	7.	685.	478.	5.	0.	0.	0.	0.
2.	0.	0.	29.	514.	178.	0.	0.	0.	0.	0.
1.	0.	0.	3.	123.	17.	0.	0.	0.	0.	0.
	1	2	3	4	5	6	7	8	9	10

U COMP

Fig. 6b Scattergram

u/v Component Wind 1 - 31 August 1971

INTERVAL NUMBER	SPEED SEP LOWER	SPEED SEP UPPER	NUMBER OF OBS	DIR SEP LOWER	DIR SEP UPPER	NUMBER OF OBS
1	0.000	2.000	211	0.000	0.523	16
2	2.000	4.000	224	0.523	1.047	162
3	4.000	6.000	257	1.047	1.570	110
4	6.000	8.000	230	1.570	2.094	139
5	8.000	10.000	242	2.094	2.618	164
6	10.000	12.000	187	2.618	3.141	176
7	12.000	14.000	186	3.141	3.664	652
8	14.000	16.000	150	3.664	4.188	287
9	16.000	18.000	120	4.188	4.711	49
10	18.000	20.000	18	4.711	5.235	4
11				5.235	5.758	12
12				5.758	6.282	54

SCATTER DIAGRAM

SPEED

10	0	0	0	0	0	0	15	3	0	0	0	0
9	0	0	0	0	0	0	74	46	0	0	0	0
8	0	0	0	0	0	0	110	40	0	0	0	0
7	1	23	17	5	0	2	123	13	2	0	0	0
6	9	50	4	9	3	6	72	26	8	0	0	0
5	2	18	14	26	17	18	89	56	2	0	0	0
4	0	31	25	26	16	36	67	24	5	0	0	0
3	0	21	9	28	45	42	64	42	5	1	0	0
2	0	11	26	29	48	51	21	13	15	1	5	4
1	4	8	15	16	35	21	17	24	12	2	7	50
	1	2	3	4	5	6	7	8	9	10	11	12

DIR

Fig. 7a Scattergram

Wind Speed/Direction 1 - 15 September 1970

INTERVAL NUMBER	U COMPSEP LOWER	U COMPSEP UPPER	NUMBER OF OBS	V COMPSEP LOWER	V COMPSEP UPPER	NUMBER OF OBS
1	-2Ø.ØØØ	-16.ØØØ	Ø	-2Ø.ØØØ	-16.ØØØ	37
2	-16.ØØØ	-12.ØØØ	1	-16.ØØØ	-12.ØØØ	293
3	-12.ØØØ	-8.ØØØ	129	-12.ØØØ	-8.ØØØ	256
4	-8.ØØØ	-4.ØØØ	387	-8.ØØØ	-4.ØØØ	4Ø4
5	-4.ØØØ	Ø.ØØØ	528	-4.ØØØ	Ø.ØØØ	467
6	Ø.ØØØ	4.ØØØ	445	Ø.ØØØ	4.ØØØ	22Ø
7	4.ØØØ	8.ØØØ	231	4.ØØØ	8.ØØØ	1Ø7
8	8.ØØØ	12.ØØØ	88	8.ØØØ	12.ØØØ	41
9	12.ØØØ	16.ØØØ	16	12.ØØØ	16.ØØØ	Ø
1Ø	16.ØØØ	2Ø.ØØØ	Ø	16.ØØØ	2Ø.ØØØ	Ø

SCATTER DIAGRAM

V COMP

1Ø.	Ø.	Ø.	Ø.	Ø.	Ø.	Ø.	Ø.	Ø.	Ø.	Ø.
9.	Ø.	Ø.	Ø.	Ø.	Ø.	Ø.	Ø.	Ø.	Ø.	Ø.
8.	Ø.	Ø.	Ø.	Ø.	Ø.	Ø.	41.	Ø.	Ø.	Ø.
7.	Ø.	Ø.	Ø.	Ø.	Ø.	9.	45.	47.	6.	Ø.
6.	Ø.	Ø.	Ø.	Ø.	58.	95.	47.	14.	6.	Ø.
5.	Ø.	Ø.	3.	19.	13Ø.	223.	67.	21.	4.	Ø.
4.	Ø.	Ø.	24.	73.	176.	96.	29.	6.	Ø.	Ø.
3.	Ø.	Ø.	41.	1Ø3.	9Ø.	2Ø.	2.	Ø.	Ø.	Ø.
2.	Ø.	1.	61.	161.	68.	2.	Ø.	Ø.	Ø.	Ø.
1.	Ø.	Ø.	Ø.	31.	6.	Ø.	Ø.	Ø.	Ø.	Ø.
	1	2	3	4	5	6	7	8	9	1Ø

U COMP

Fig. 7b Scattergram

U/V Component Winds 1 - 15 September 1970.

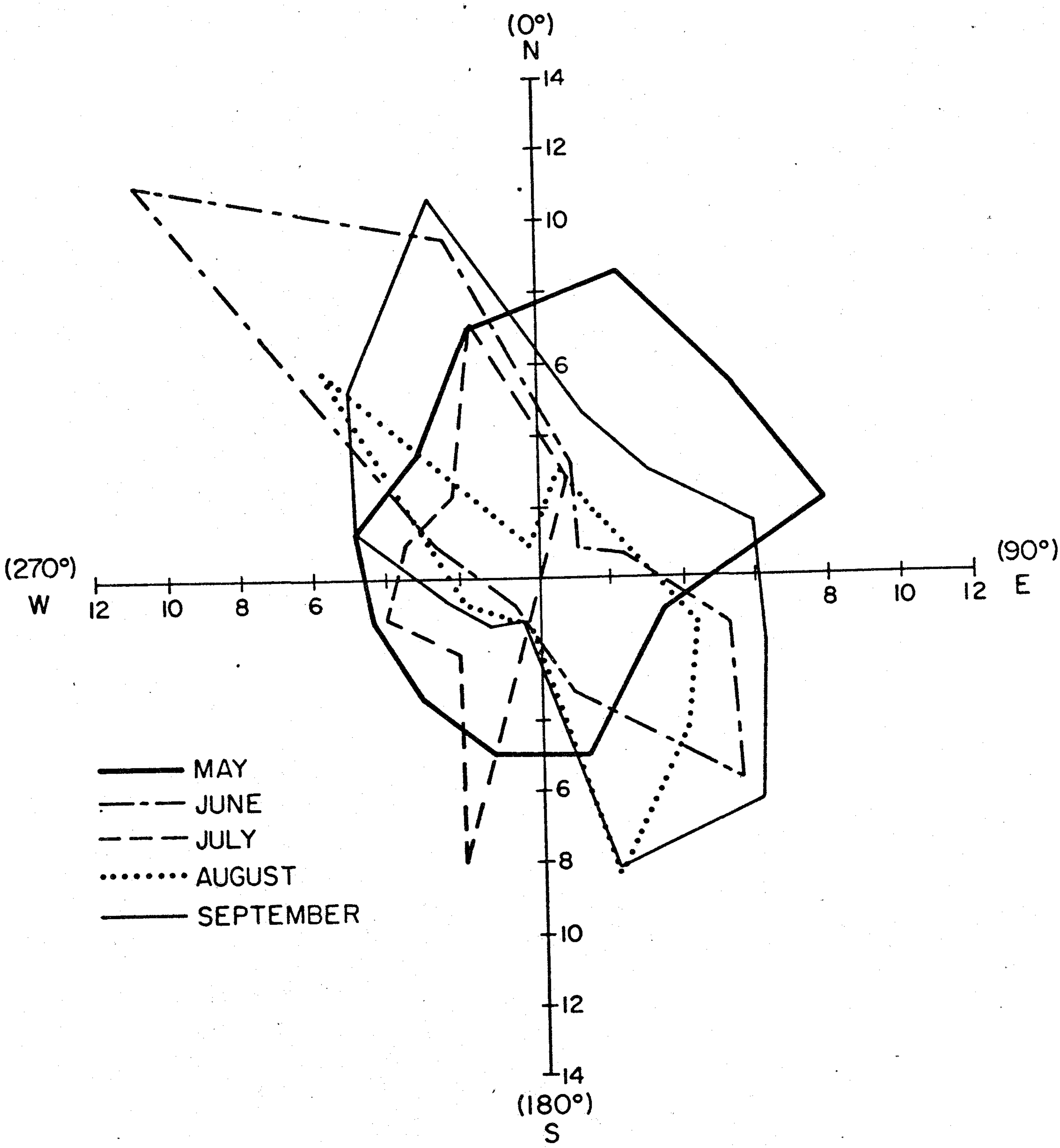

Figure 8. Plot of mean monthly wind speeds against direction. Directions are true. Direction intervals are 30°.

INTERVAL NUMBER	SPEED CM LOWER	SPEED CM UPPER	NUMBER OF OBS	DIR AG C LOWER	DIR AG C UPPER	NUMBER OF OBS
1	0	.050	67	0	.524	9
2	.050	.100	152	.524	1.047	27
3	.100	.150	279	1.047	1.570	32
4	.150	.200	293	1.570	2.094	43
5	.200	.250	295	2.094	2.617	133
6	.250	.300	165	2.617	3.141	315
7	.300	.350	37	3.141	3.664	408
8	.350	.400	28	3.664	4.188	227
9	.400	.450	12	4.188	4.711	78
10	.450	.500	0	4.711	5.235	30
11				5.235	5.758	23
12				5.758	6.282	3

SCATTER DIAGRAM

SPEED												
10	0	0	0	0	0	0	0	0	0	0	0	0
9	0	0	0	0	0	0	2	10	0	0	0	0
8	0	0	0	0	0	3	17	8	0	0	0	0
7	0	0	0	0	0	10	19	8	0	0	0	0
6	0	0	3	5	12	70	50	25	0	0	0	0
5	0	3	12	25	51	62	89	50	3	0	0	0
4	0	7	13	7	42	72	95	39	18	0	0	0
3	0	12	1	1	23	70	89	42	33	7	1	0
2	6	4	3	5	2	22	37	39	13	10	9	2
1	3	1	0	0	3	6	10	6	11	13	13	1
	1	2	3	4	5	6	7	8	9	10	11	12
	DIR											

Fig. 9a. Scattergram

Current Speed/Direction 5 - 14 August 1970.

INTERVAL NUMBER	U COMPC LOWER	U COMPC UPPER	NUMBER OF OBS	V COMPC LOWER	V COMPC UPPER	NUMBER OF OBS
1	-Ø.5ØØ	-Ø.4ØØ	Ø	-Ø.5ØØ	-Ø.4ØØ	Ø
2	-Ø.4ØØ	-Ø.3ØØ	5	-Ø.4ØØ	-Ø.3ØØ	54
3	-Ø.3ØØ	-Ø.2ØØ	19	-Ø.3ØØ	-Ø.2ØØ	29Ø
4	-Ø.2ØØ	-Ø.1ØØ	216	-Ø.2ØØ	-Ø.1ØØ	569
5	-Ø.1ØØ	Ø	529	-Ø.1ØØ	Ø	29Ø
6	Ø	.1ØØ	362	Ø	.1ØØ	117
7	.1ØØ	.2ØØ	161	.1ØØ	.2ØØ	8
8	.2ØØ	.3ØØ	36	.2ØØ	.3ØØ	Ø
9	.3ØØ	.4ØØ	Ø	.3ØØ	.4ØØ	Ø
1Ø	.4ØØ	.5ØØ	Ø	.4ØØ	.5ØØ	Ø

SCATTER DIAGRAM

V COMP

1Ø.	Ø.	Ø.	Ø.	Ø.	Ø.	Ø.	Ø.	Ø.	Ø.	Ø.
9.	Ø.	Ø.	Ø.	Ø.	Ø.	Ø.	Ø.	Ø.	Ø.	Ø.
8.	Ø.	Ø.	Ø.	Ø.	Ø.	Ø.	Ø.	Ø.	Ø.	Ø.
7.	Ø.	Ø.	Ø.	Ø.	Ø.	Ø.	8.	Ø.	Ø.	Ø.
6.	Ø.	Ø.	Ø.	5.	52.	26.	21.	13.	Ø.	Ø.
5.	Ø.	Ø.	Ø.	56.	144.	48.	2Ø.	22.	Ø.	Ø.
4.	Ø.	Ø.	5.	8Ø.	225.	176.	82.	1.	Ø.	Ø.
3.	Ø.	3.	8.	58.	9Ø.	1Ø1.	3Ø.	Ø.	Ø.	Ø.
2.	Ø.	2.	6.	17.	18.	11.	Ø.	Ø.	Ø.	Ø.
1.	Ø.	Ø.	Ø.	Ø.	Ø.	Ø.	Ø.	Ø.	Ø.	Ø.
	1	2	3	4	5	6	7	8	9	1Ø

U COMP

Fig. 9b Scattergram
U/V Components of Current 5 - 14 August 1970

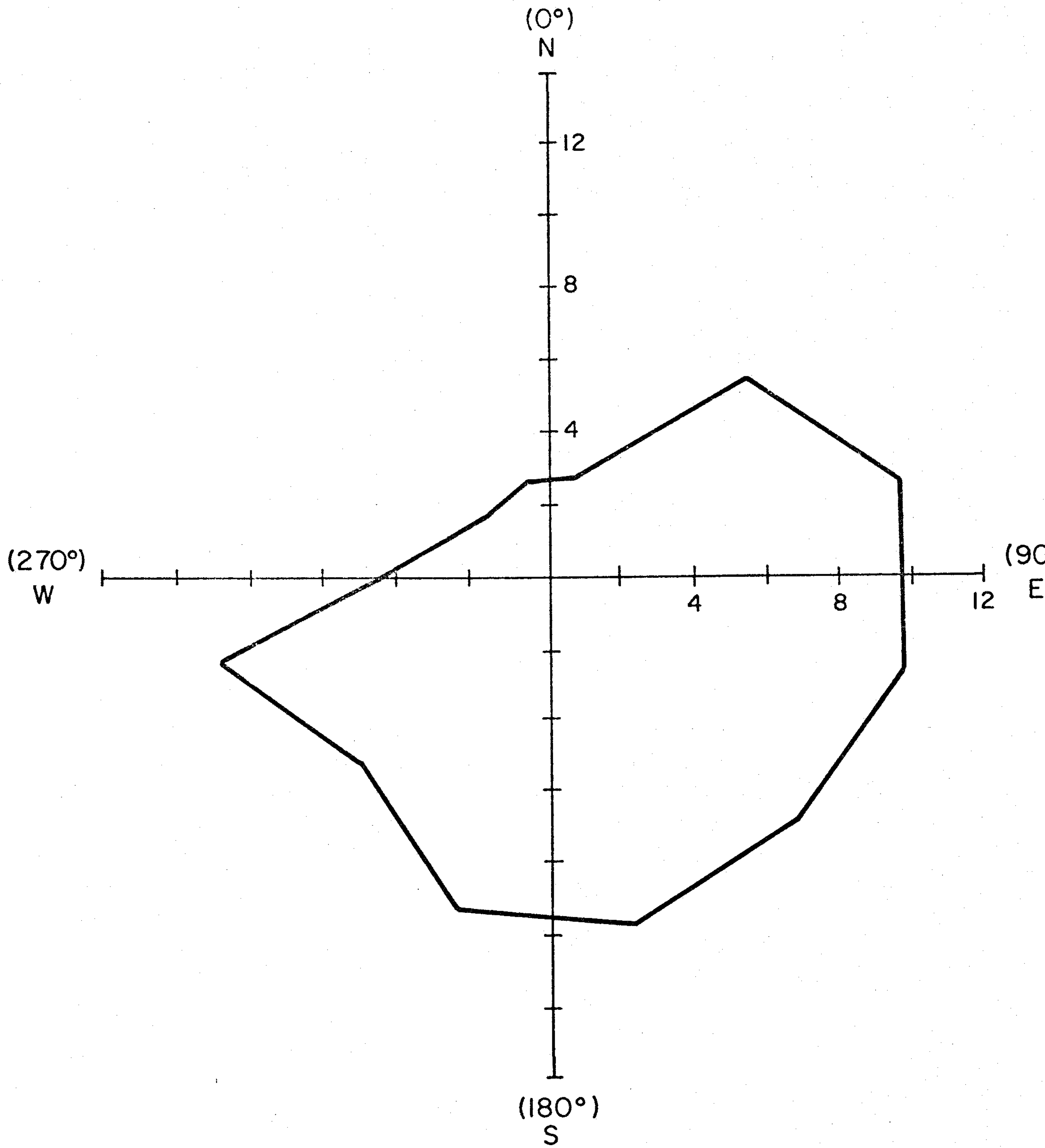

Figure 9c. Mean Current Speed vs Direction for August 5 - 14.

INTERVAL NUMBER	SPEEDAGC LOWER	SPEEDAGC UPPER	NUMBER OF OBS	DIRAGWDC LOWER	DIRAGWDC UPPER	NUMBER OF OBS
1	0	2.000	44	0	.524	232
2	2.000	4.000	155	.524	1.047	171
3	4.000	6.000	216	1.047	1.570	30
4	6.000	8.000	279	1.570	2.094	14
5	8.000	10.000	185	2.094	2.617	22
6	10.000	12.000	128	2.617	3.141	49
7	12.000	14.000	182	3.141	3.664	617
8	14.000	16.000	70	3.664	4.188	154
9	16.000	18.000	63	4.188	4.711	10
10	18.000	20.000	6	4.711	5.235	7
11				5.235	5.758	6
12				5.758	6.282	16

SCATTER DIAGRAM

SPEED

10.	0.	0.	0.	0.	0.	0.	6.	0.	0.	0.	0.	0.
9.	0.	0.	0.	0.	0.	0.	58.	5.	0.	0.	0.	0.
8.	4.	0.	0.	0.	0.	0.	66.	0.	0.	0.	0.	0.
7.	45.	0.	0.	0.	0.	0.	80.	57.	0.	0.	0.	0.
6.	35.	5.	0.	0.	0.	0.	70.	18.	0.	0.	0.	0.
5.	63.	26.	5.	0.	0.	0.	85.	6.	0.	0.	0.	0.
4.	54.	94.	12.	1.	0.	1.	99.	17.	1.	0.	0.	0.
3.	26.	35.	12.	2.	0.	23.	83.	32.	3.	0.	0.	0.
2.	0.	9.	1.	11.	22.	24.	62.	13.	4.	6.	3.	0.
1.	5.	2.	0.	0.	0.	1.	8.	6.	2.	1.	3.	16.
	1	2	3	4	5	6	7	8	9	10	11	12

DIR

Fig. 10a Scattergram

Wind Speed/Direction 5 - 14 August

INTERVAL NUMBER	U CCOM A LOWER	U CCOM A UPPER	NUMBER OF OBS	V COMP A LOWER	V COMP A UPPER	NUMBER OF OBS
1	-20.000	-16.000	0	-20.000	-16.000	15
2	-16.000	-12.000	0	-16.000	-12.000	145
3	-12.000	-8.000	19	-12.000	-8.000	262
4	-8.000	-4.000	352	-8.000	-4.000	251
5	-4.000	0	437	-4.000	0	193
6	0	4.000	342	0	4.000	100
7	4.000	8.000	175	4.000	8.000	234
8	8.000	12.000	3	8.000	12.000	93
9	12.000	16.000	0	12.000	16.000	35
10	16.000	20.000	0	16.000	20.000	0

SCATTER DIAGRAM

V COMP

V COMP \ U CCOM	1	2	3	4	5	6	7	8	9	10
10	0	0	0	0	0	0	0	0	0	0
9	0	0	0	0	0	31	4	0	0	0
8	0	0	0	0	0	39	54	0	0	0
7	0	0	0	0	0	150	84	0	0	0
6	0	0	0	0	27	39	31	3	0	0
5	0	0	0	8	124	59	2	0	0	0
4	0	0	0	21	206	24	0	0	0	0
3	0	0	0	187	75	0	0	0	0	0
2	0	0	16	124	5	0	0	0	0	0
1	0	0	3	12	0	0	0	0	0	0

U CCOM

<u>Fig. 10b</u> Scattergram
Wind U/V components August 5-14, 1970

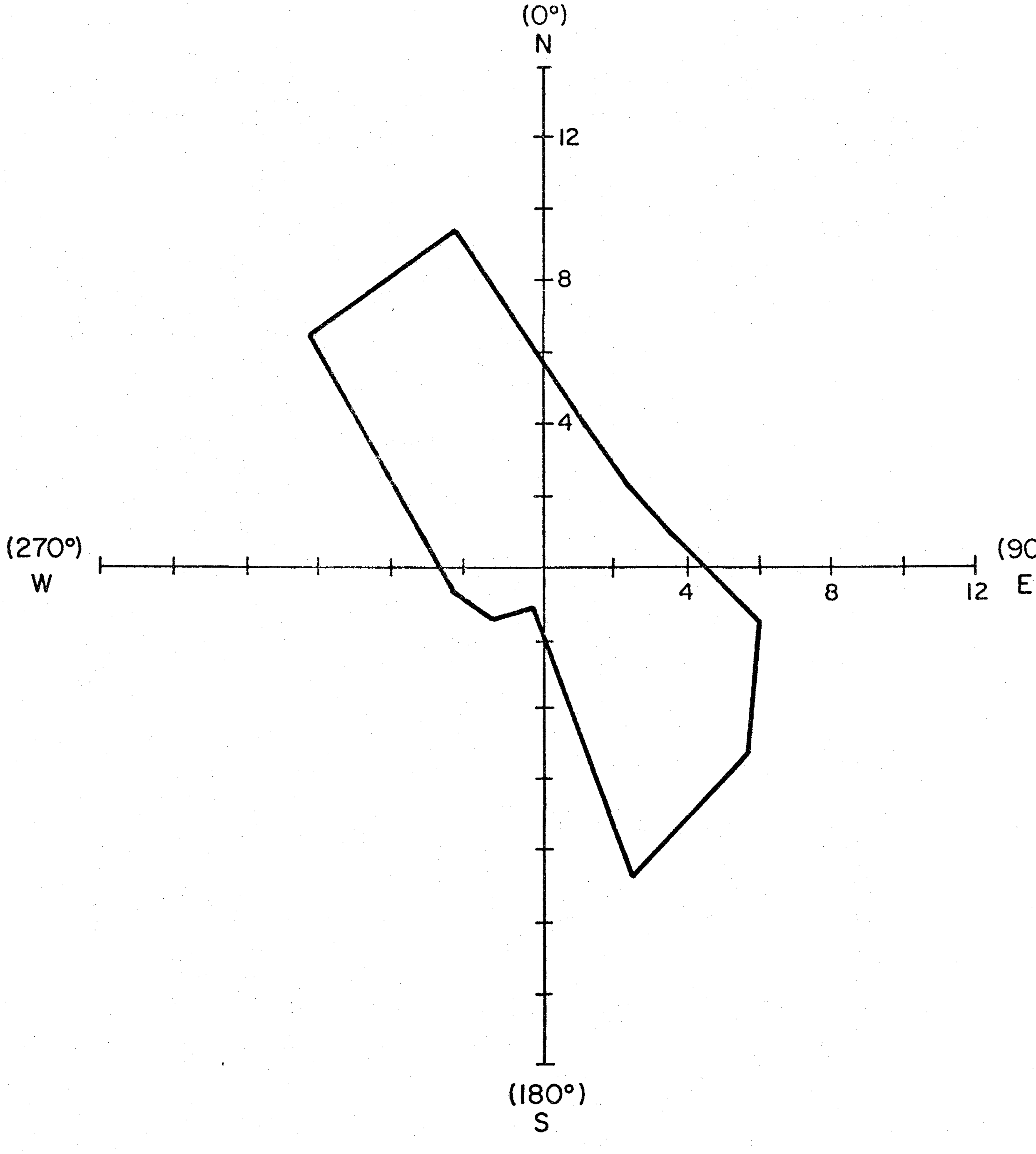

Figure 10c. Mean Wind Speed vs direction for August 5 - 14.

INTERVAL NUMBER	SPEED CM LOWER	SPEED CM UPPER	NUMBER OF OBS	DIR AG C LOWER	DIR AG C UPPER	NUMBER OF OBS
1	0	.050	67	0	.524	9
2	.050	.100	152	.524	1.047	27
3	.100	.150	279	1.047	1.570	32
4	.150	.200	293	1.570	2.094	43
5	.200	.250	295	2.094	2.617	133
6	.250	.300	165	2.617	3.141	315
7	.300	.350	37	3.141	3.664	408
8	.350	.400	28	3.664	4.188	227
9	.400	.450	12	4.188	4.711	78
10	.450	.500	0	4.711	5.235	30
11				5.235	5.758	23
12				5.758	6.282	3

SCATTER DIAGRAM

SPEED

10	0	0	0	0	0	0	0	0	0	0	0	0
9	0	0	0	0	0	0	2	10	0	0	0	0
8	0	0	0	0	0	3	17	8	0	0	0	0
7	0	0	0	0	0	10	19	8	0	0	0	0
6	0	0	3	5	12	70	50	25	0	0	0	0
5	0	3	12	25	51	62	89	50	3	0	0	0
4	0	7	13	7	42	72	95	39	18	0	0	0
3	0	12	1	1	23	70	89	42	33	7	1	0
2	6	4	3	5	2	22	37	39	13	10	9	2
1	3	1	0	0	3	6	10	6	11	13	13	1
	1	2	3	4	5	6	7	8	9	10	11	12

DIR

Fig. 11a Scattergram

Wind Speed/Current Direction

5 - 14 August 1970

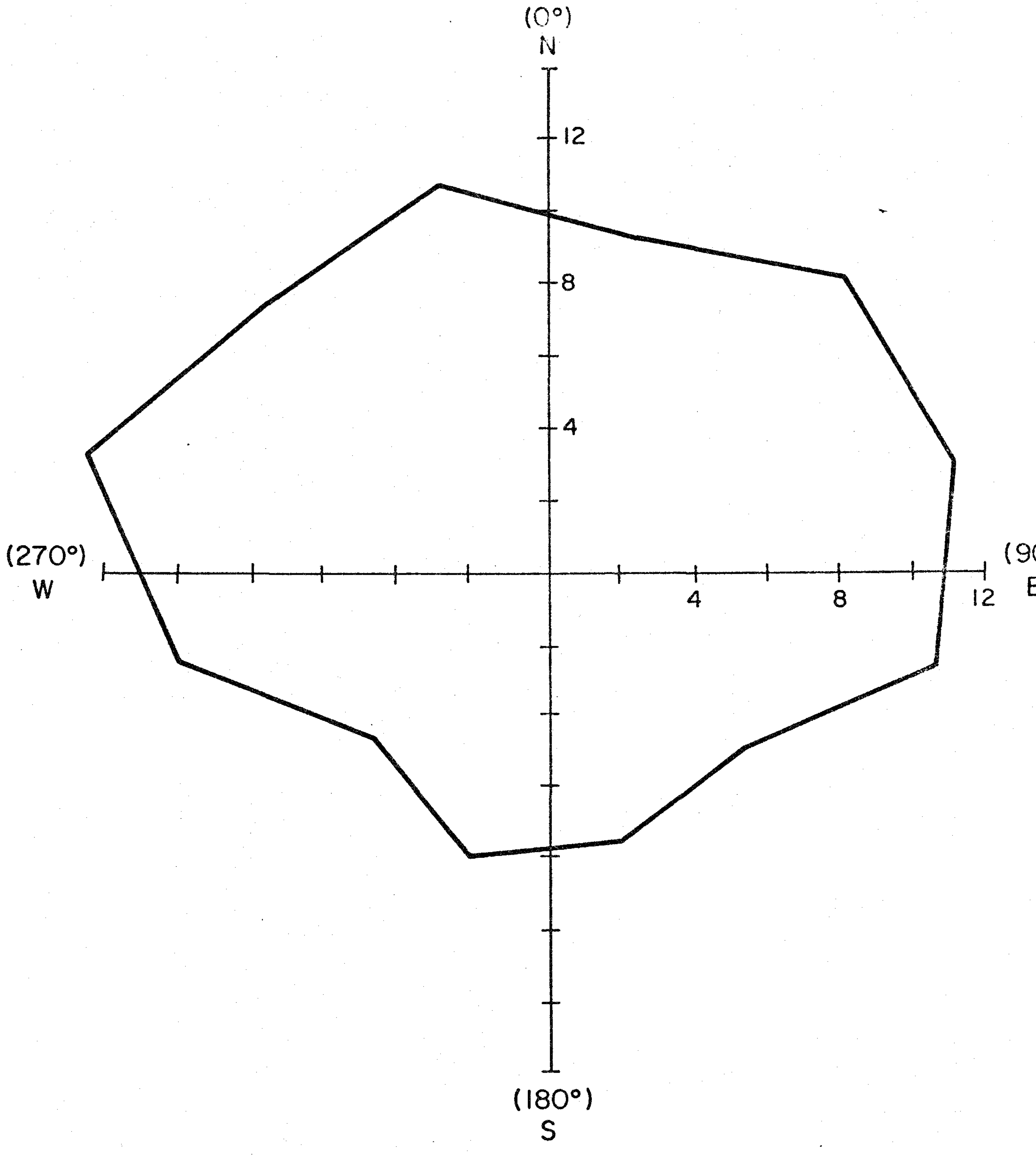

Figure 11b. Mean Wind Speed vs Current Direction for August 5 - 14.

INTERVAL NUMBER	CM DR AG LOWER	CM DR AG UPPER	NUMBER OF OBS	WD DR AG LOWER	WD DR AG UPPER	NUMBER OF OBS
1	0	.524	9	0	.524	232
2	.524	1.047	27	.524	1.048	171
3	1.047	1.570	32	1.048	1.572	30
4	1.570	2.094	43	1.572	2.096	14
5	2.094	2.617	133	2.096	2.620	22
6	2.617	3.141	315	2.620	3.144	49
7	3.141	3.664	408	3.144	3.668	621
8	3.664	4.188	227	3.668	4.192	150
9	4.188	4.711	78	4.192	4.716	10
10	4.711	5.235	30	4.716	5.240	8
11	5.235	5.758	23	5.240	5.764	5
12	5.758	6.282	3	5.764	6.288	16

SCATTER DIAGRAM

WD DR

12.	0.	0.	0.	6.	10.	0.	0.	0.	0.	0.	0.	0.
11.	0.	0.	0.	0.	5.	0.	0.	0.	0.	0.	0.	0.
10.	0.	0.	0.	0.	4.	4.	0.	0.	0.	0.	0.	0.
9.	0.	0.	0.	1.	0.	6.	3.	0.	0.	0.	0.	0.
8.	2.	0.	1.	1.	17.	32.	46.	12.	27.	8.	4.	0.
7.	0.	11.	13.	15.	47.	101.	246.	132.	37.	14.	4.	1.
6.	0.	0.	0.	0.	0.	1.	13.	35.	0.	0.	0.	0.
5.	0.	0.	0.	0.	0.	16.	6.	0.	0.	0.	0.	0.
4.	0.	0.	0.	0.	2.	10.	0.	2.	0.	0.	0.	0.
3.	0.	7.	4.	0.	0.	6.	4.	9.	0.	0.	0.	0.
2.	6.	5.	5.	1.	18.	53.	37.	36.	2.	0.	6.	2.
1.	1.	4.	9.	19.	30.	86.	53.	1.	12.	8.	9.	0.
	1	2	3	4	5	6	7	8	9	10	11	12

CM DR

Fig. 11c. Scattergram

INTERVAL NUMBER	CM SP AG LOWER	CM SP AG UPPER	NUMBER OF OBS	WD SP AG LOWER	WD SP AG UPPER	NUMBER OF OBS
1	0	.050	67	0	2.000	44
2	.050	.100	152	2.000	4.000	155
3	.100	.150	279	4.000	6.000	216
4	.150	.200	293	6.000	8.000	279
5	.200	.250	295	8.000	10.000	185
6	.250	.300	165	10.000	12.000	128
7	.300	.350	37	12.000	14.000	182
8	.350	.400	28	14.000	16.000	70
9	.400	.450	12	16.000	18.000	63
10	.450	.500	0	18.000	20.000	6

SCATTER DIAGRAM
WD SP

WD SP	1	2	3	4	5	6	7	8	9	10
10	0	0	4	2	0	0	0	0	0	0
9	8	14	16	16	9	0	0	0	0	0
8	17	7	5	14	27	0	0	0	0	0
7	8	26	70	34	41	3	0	0	0	0
6	4	19	24	31	24	20	4	2	0	0
5	18	16	36	28	39	31	6	9	2	0
4	9	33	50	38	67	56	17	3	6	0
3	2	8	39	73	50	31	3	6	4	0
2	1	22	27	31	35	24	7	8	0	0
1	0	7	8	26	3	0	0	0	0	0

CM SP

Fig. 11d. Scattergram

Wind Speed/Current Speed August 5 - 14

D. Progressive Vector Diagrams

Progressive vector diagrams[10] of the winds and currents are shown in Figs. 12 through 16. In these figures the line is created by the addition of successive velocity vectors on the geographic plane. If spatial variations in the velocity field were negligible, the line would represent the path-history of a balloon (or drogue) which was released from Totem at the beginning of the record and which remained at anemometer (or current meter) height after release. The dots along each line would represent the location of the balloon at 2400 hours (PDT) during successive days. Fig. 13 also includes a progressive vector diagram of the current at 7 m depth during part of August. In this figure the 90° change in mean current direction after 8 August appears to be related to the 180° change in wind direction that occurred 7 August.

E. Time Series Plots

Plots[11] of the digitized wind speed, and u- and v-components, vs. time are shown in Figs. 17, 18 and 19. Also shown in Figure 18 are plots of the current at 7 m depth during August.

F. Spectral Analysis

Spectral Analysis was performed on hourly interval wind speed and u- and v-component series that were created by block-averaging ten-min interval series. The following segments of the series were analyzed separately:

16 May through 6 June
17 July through 31 July
1 August through 31 August
1 September through 20 September

ARAND[12] programs were used to estimate the autocorrelation functions and spectral densities of these segments. For each segment three truncation points were used to obtain three estimates of the spectrum having different bandwidths and confidence intervals.[13] In order to make the set of bandwidths for all segments similar, it was necessary to use different sets of truncation points as the segments are of different lengths. The autocorrelation and spectral density estimates for each segment are shown in Figs. 20 through 40. The horizontal and vertical bars on the spectral estimates indicate the bandwidth and 95% confidence interval, respectively.

---

[10] Themis Program: #CW PLOT

[11] Themis Program: #WND PLT

[12] ARAND Program: #TSPCTIC

[13] This is the window closing technique discussed by Jenkins and Watts: Spectral Analysis and its Application, Holden-Day, 1969, pp. 280-282.

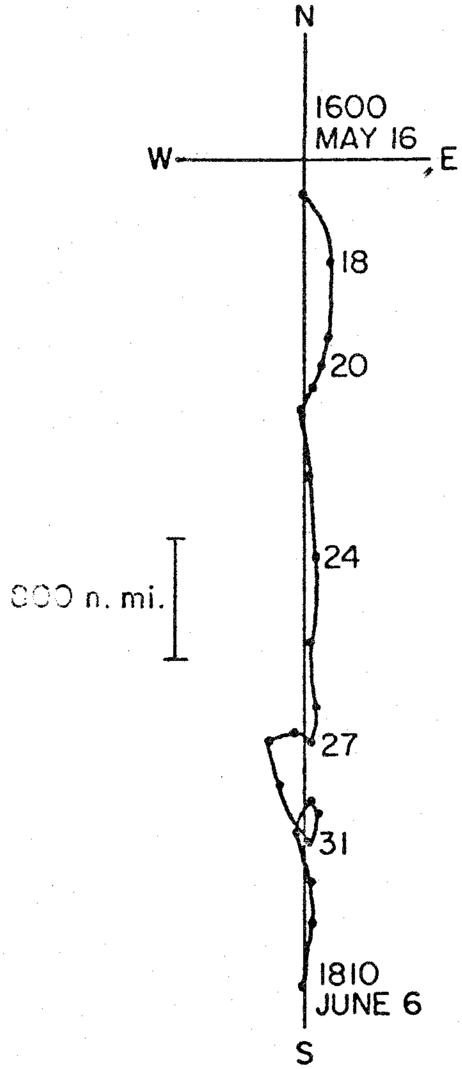

Figure 12. Progressive Vector Diagram (PVD) of Totem Winds May 16 - June 6.

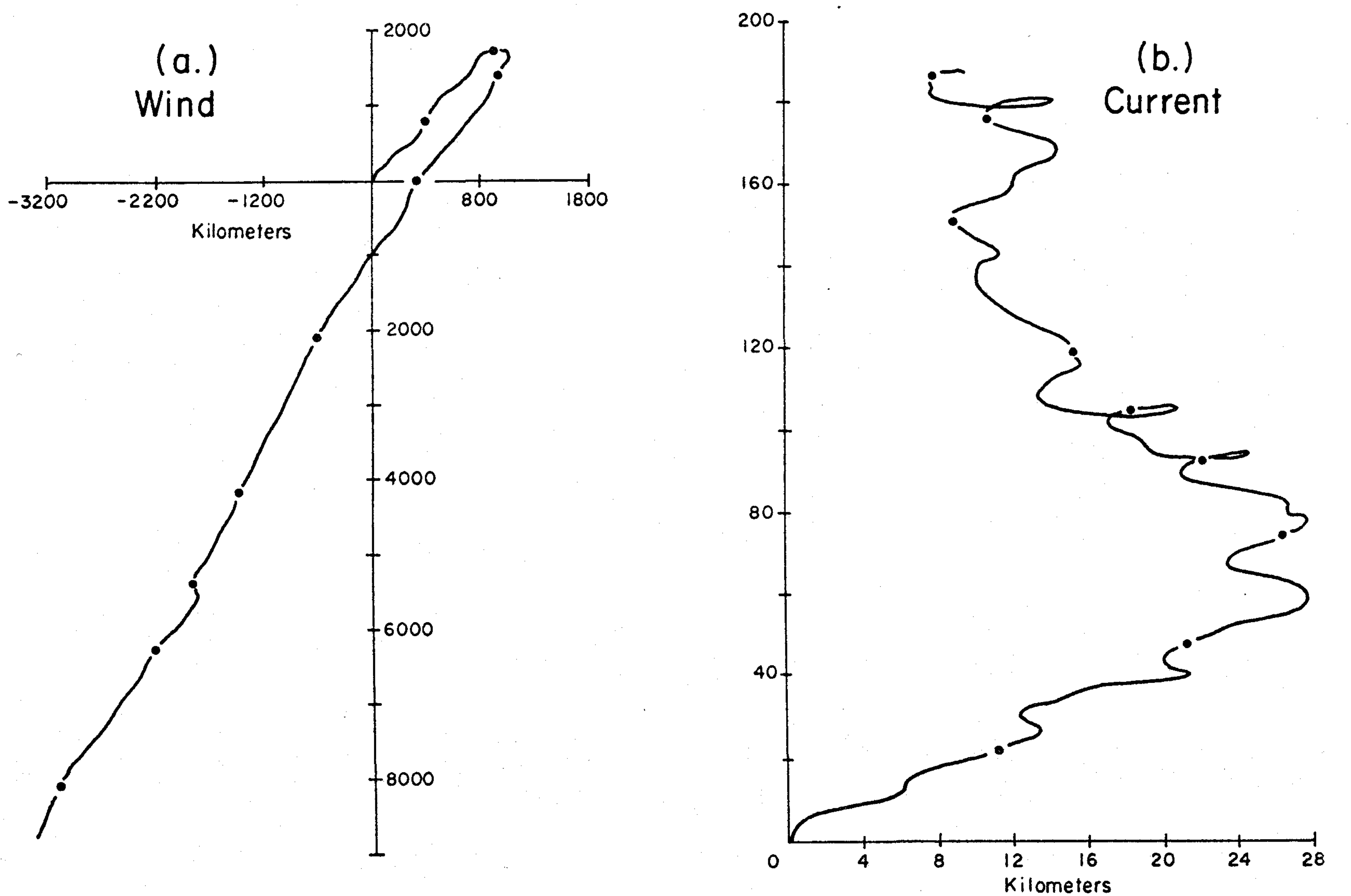

Figure 13. Progressive vector diagrams (in km) for a) wind at 10 meters height MSL and b) current at -7 meters depth MSL measured at TOTEM from 1127 August 5 to 1917 August 14, 1970. Points represent 2400 hours in successive days.

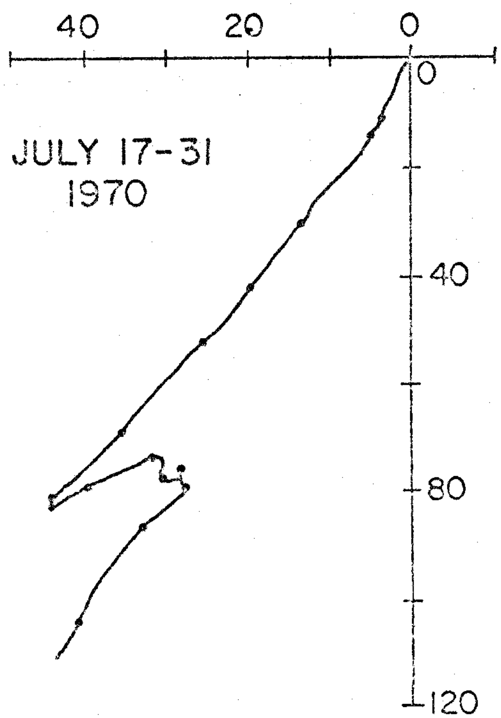

Figure 14. Progressive vector diagram (in Km) of wind at ten meters height at Totem from July 17-31, 1970. Points represent 2400 hours on successive days.

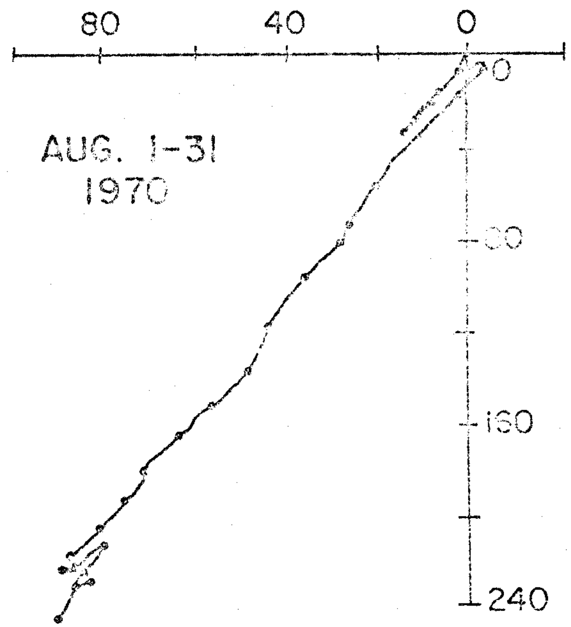

Figure 15. Progressive vector diagram (in Km) of wind at ten meters height at Totem. From August 1-31, 1970.

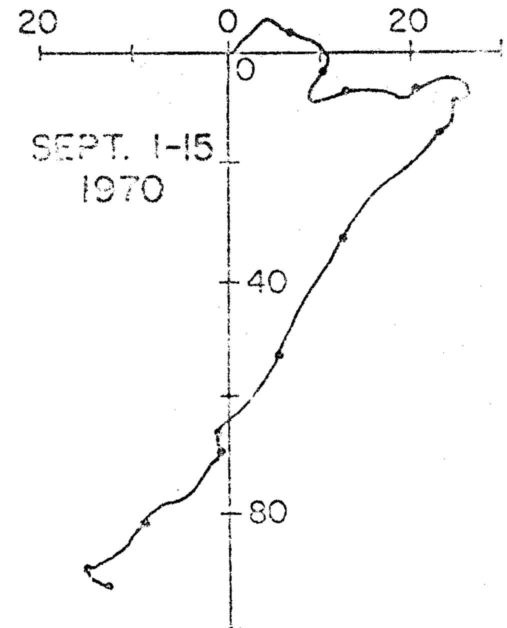

Figure 16. Progressive vector diagram (in Km) of wind at ten meters height at Totem from 0950 Sept 1 - 1400 Sept 15, 1970. Points represent 2400 hours on successive days.

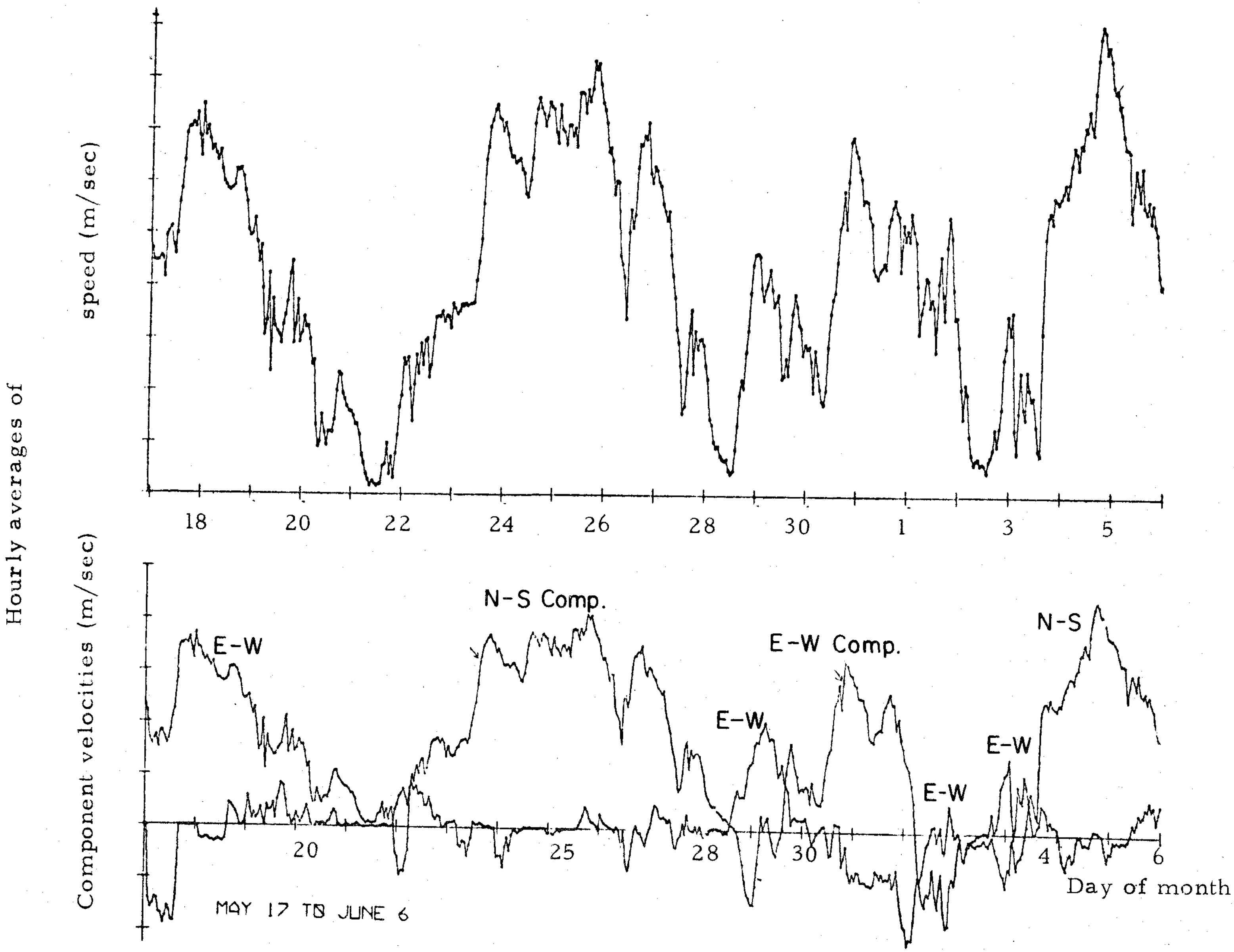

Fig. 17. Totem I wind speed and component velocities vs time (day of month).

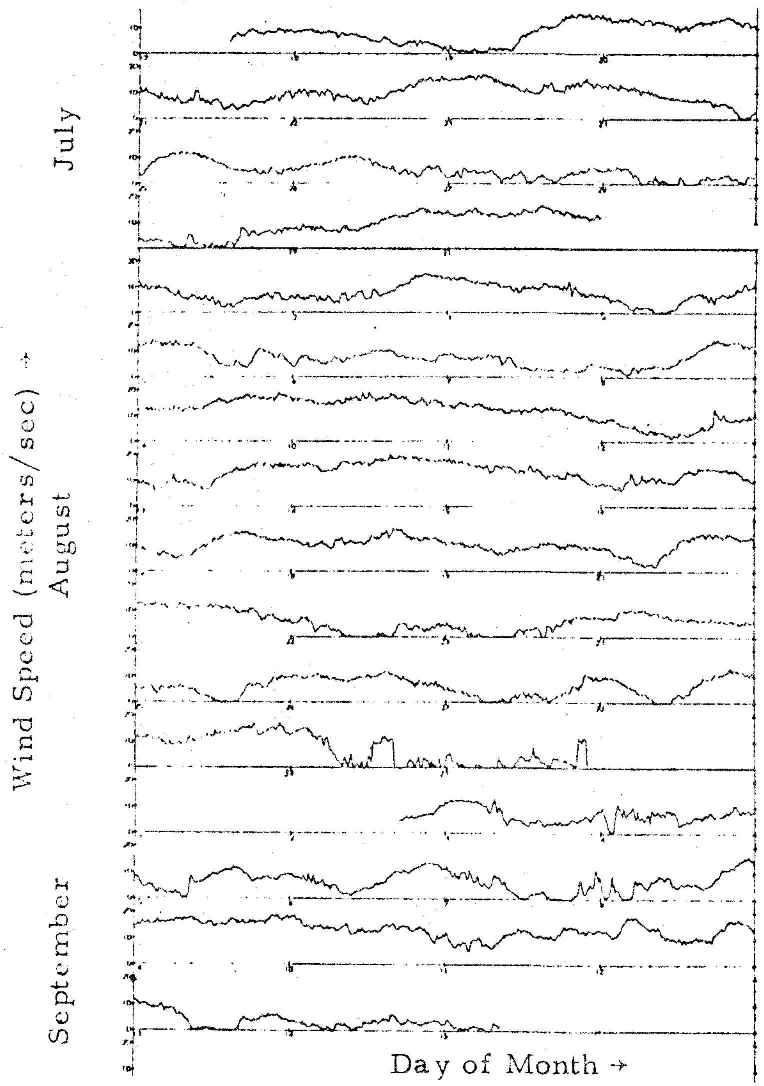

Totem wind speed, from 1350 July 17 to 0900 Sept. 15, 1970 at 10 meter height.

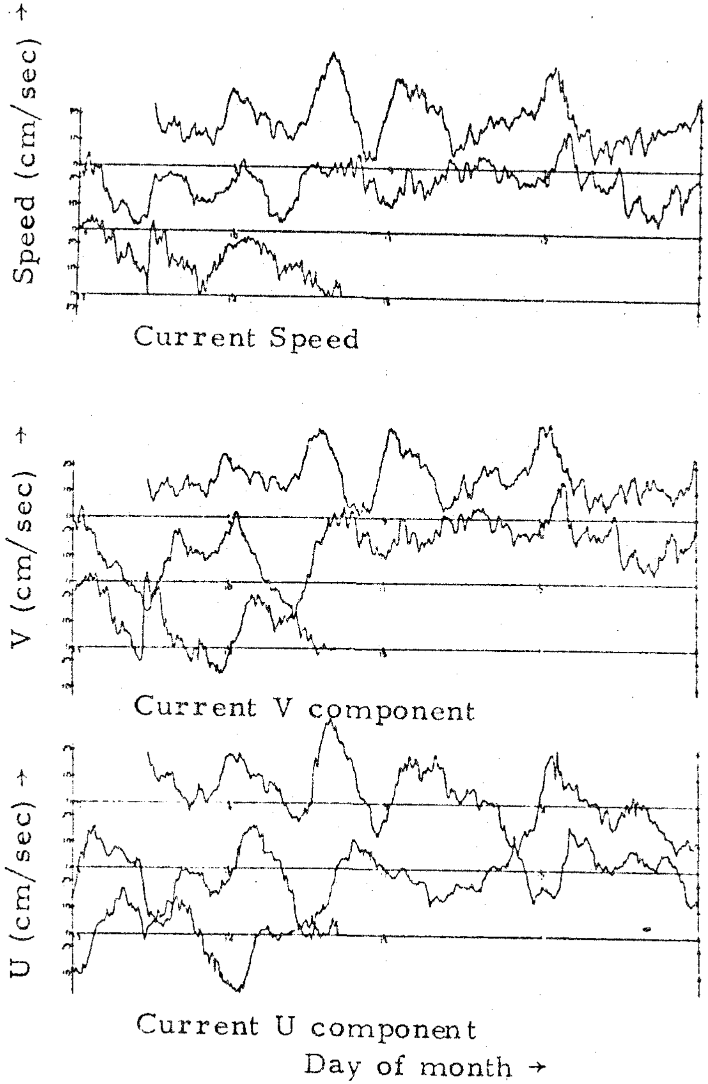

Totem current speed, U and V components, from 1132 Aug. 5 to Aug 14, 1970 at -7 meter depth

Fig. 18

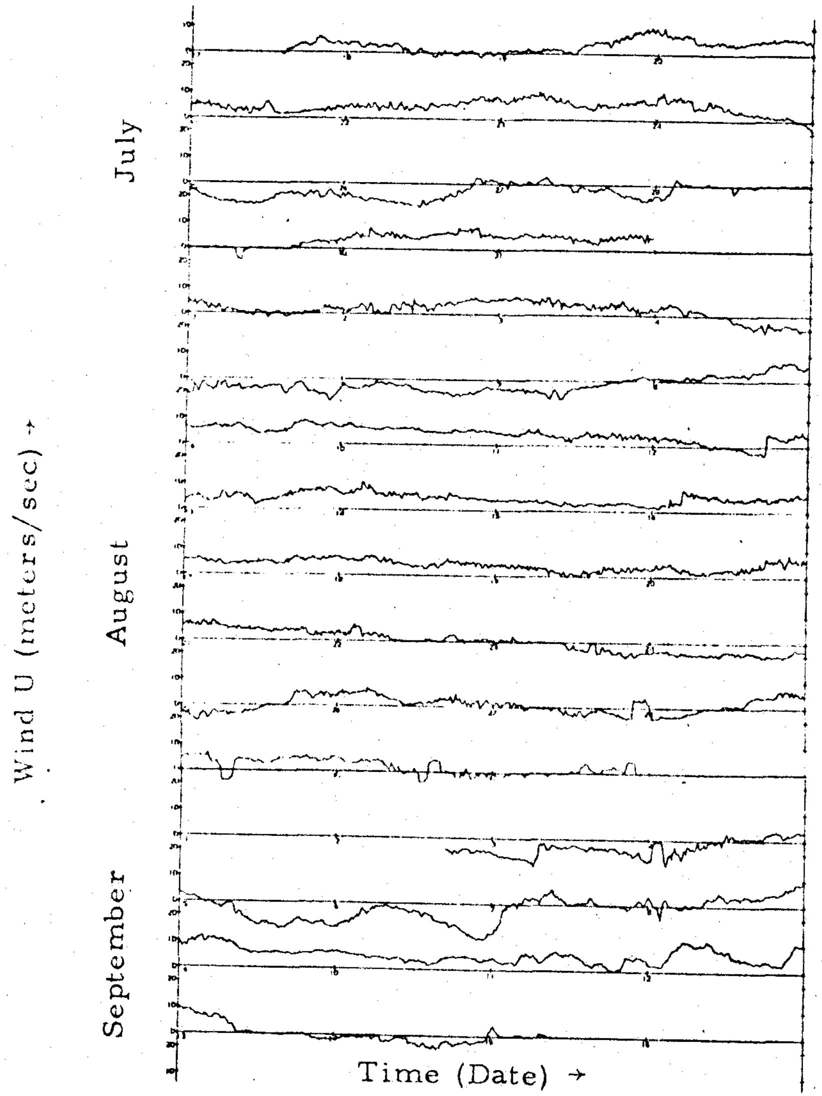

Totem wind U component from 1350 July 17 to 0900 Sept 15, 1970.

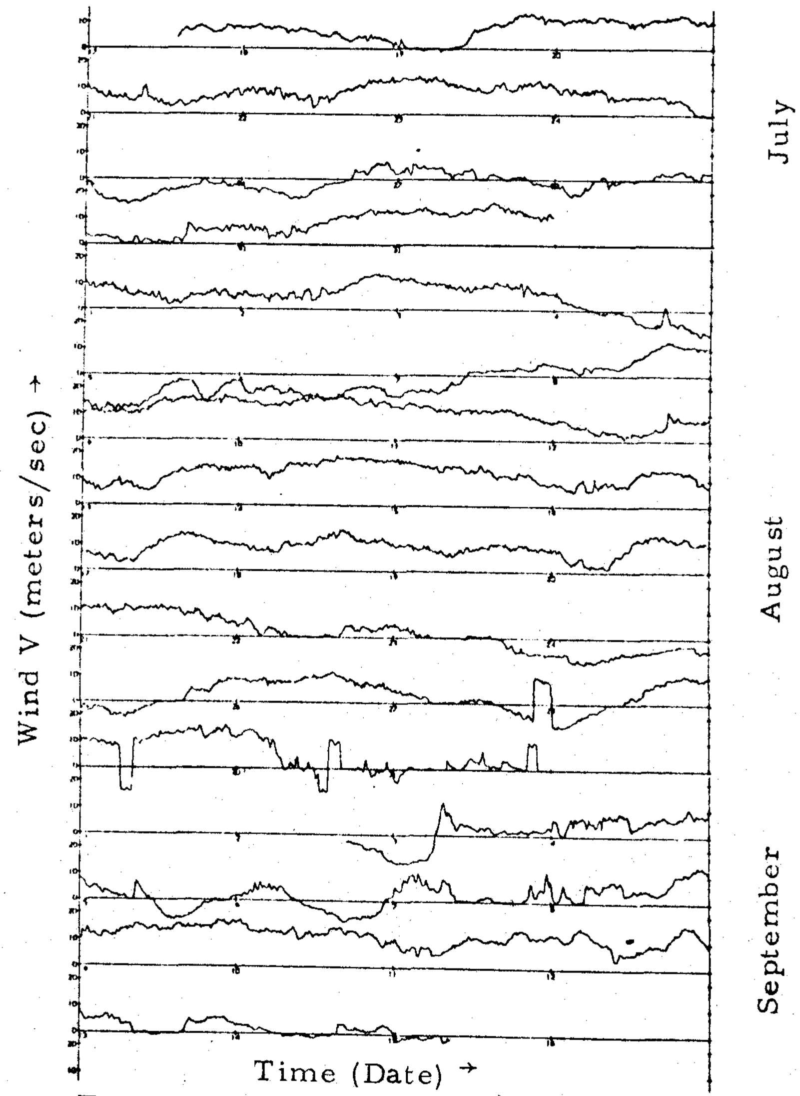

Totem wind V component from 1350 July 17 to 0900 Sept. 15, 1970.

Figure 19

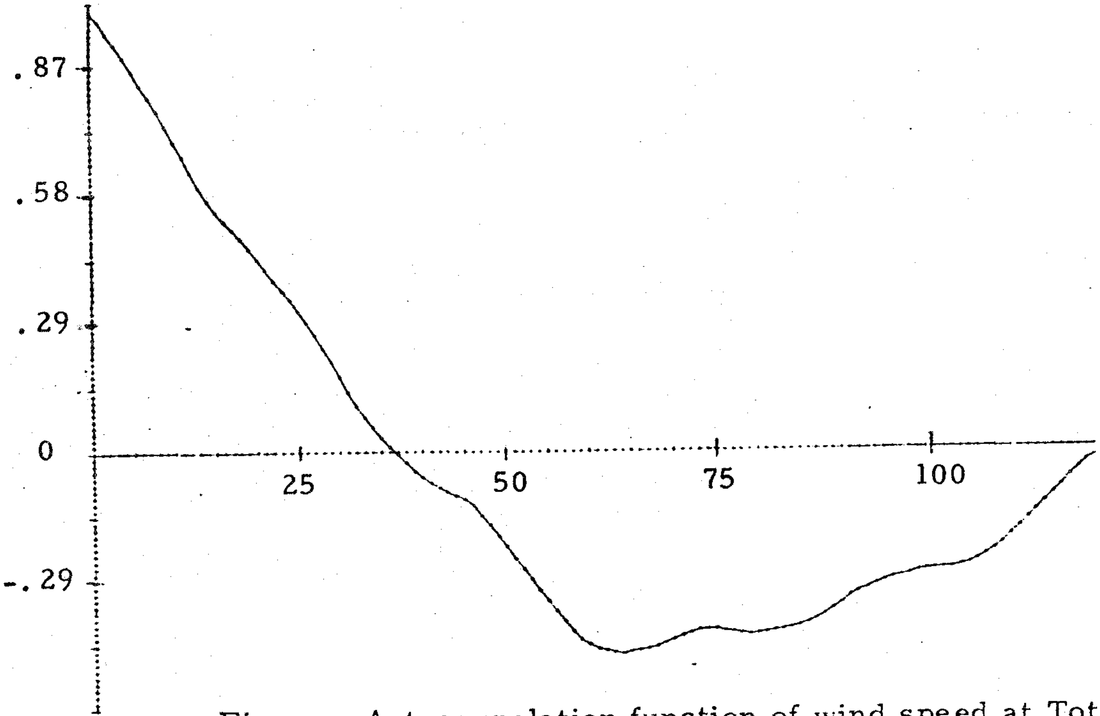

Fig. 20 Autocorrelation function of wind speed at Totem for May 16-June 6, 1970. (121 lags.)

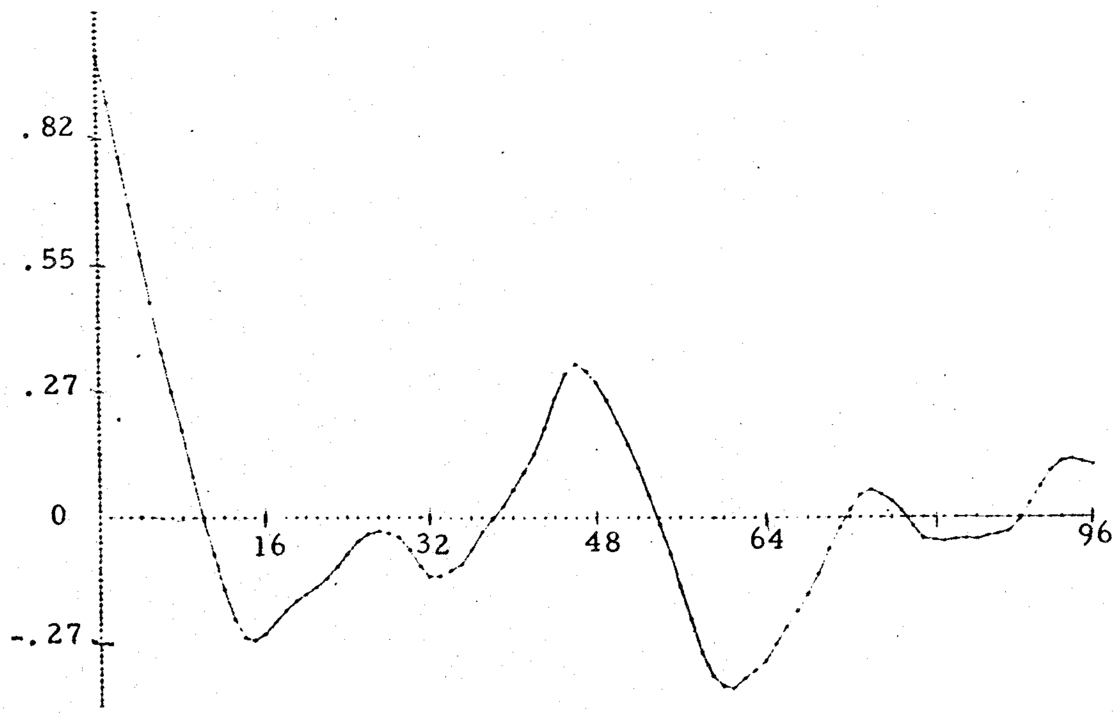

Fig. 21 Autocorrelation function of high frequency filtered wind speed at Totem for May 16-June 6, 1970. (121 lags.)

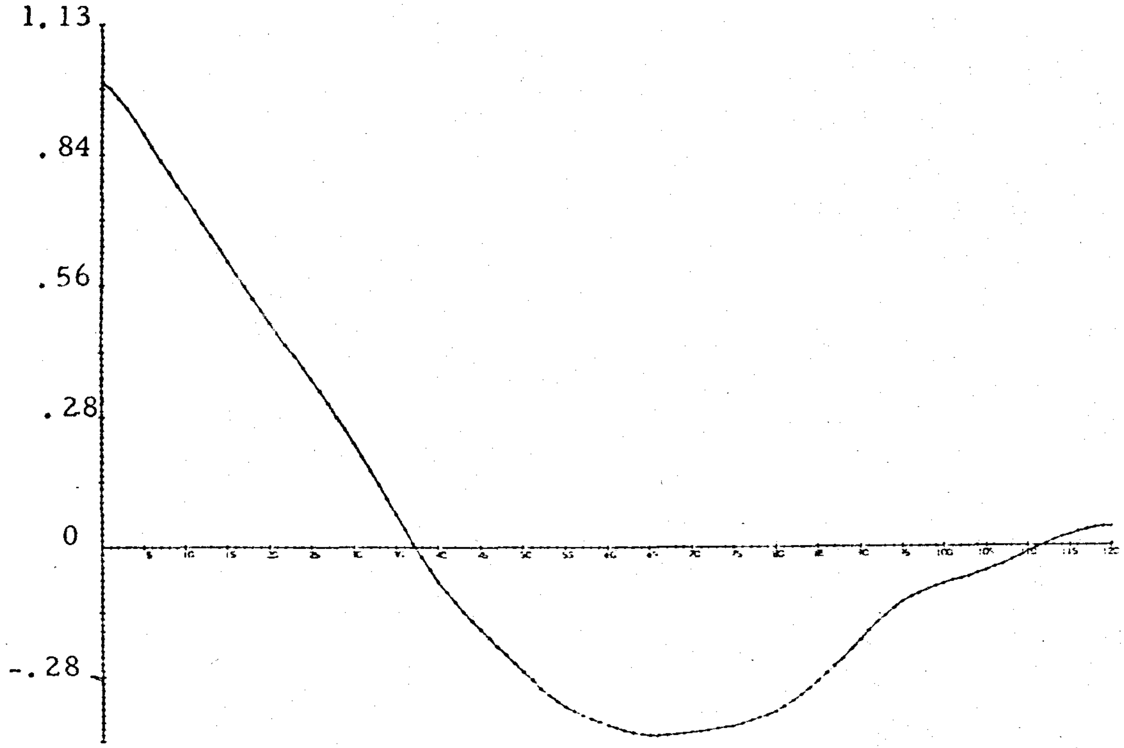

Fig. 22 Autocorrelation function of the north-south wind component velocity at Totem for May 16-June 6, 1970. (121 lags.)

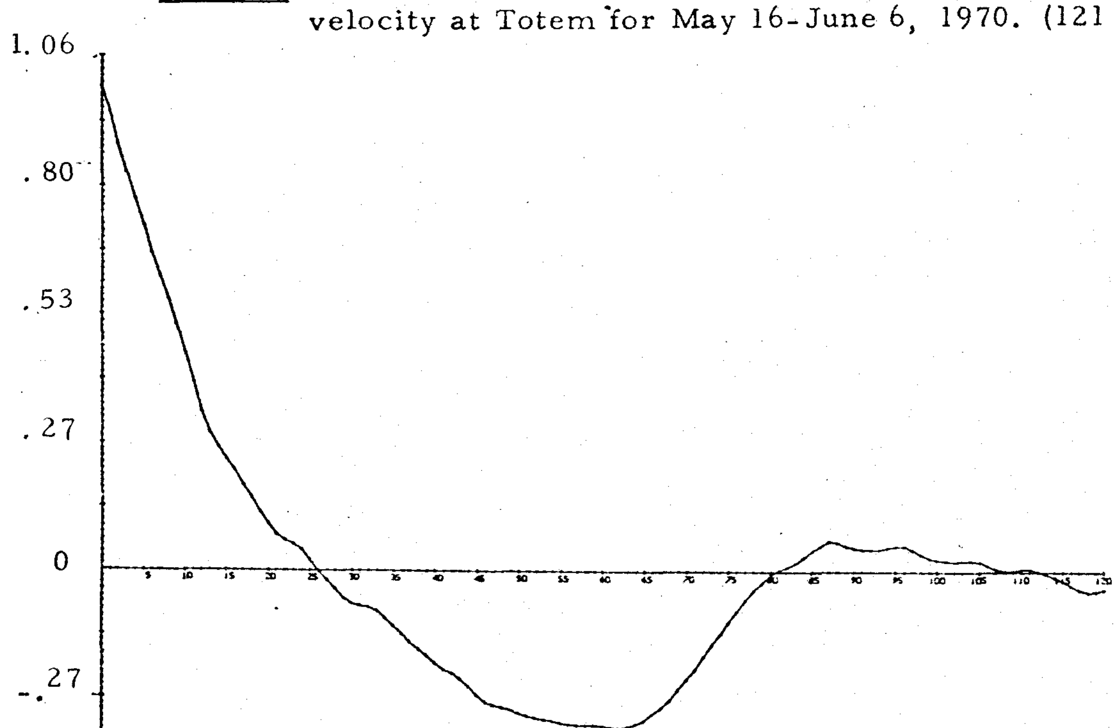

Fig. 23. Autocorrelation function of the east-west wind component velocity at Totem for May 16-June 6, 1970. (121 lags.)

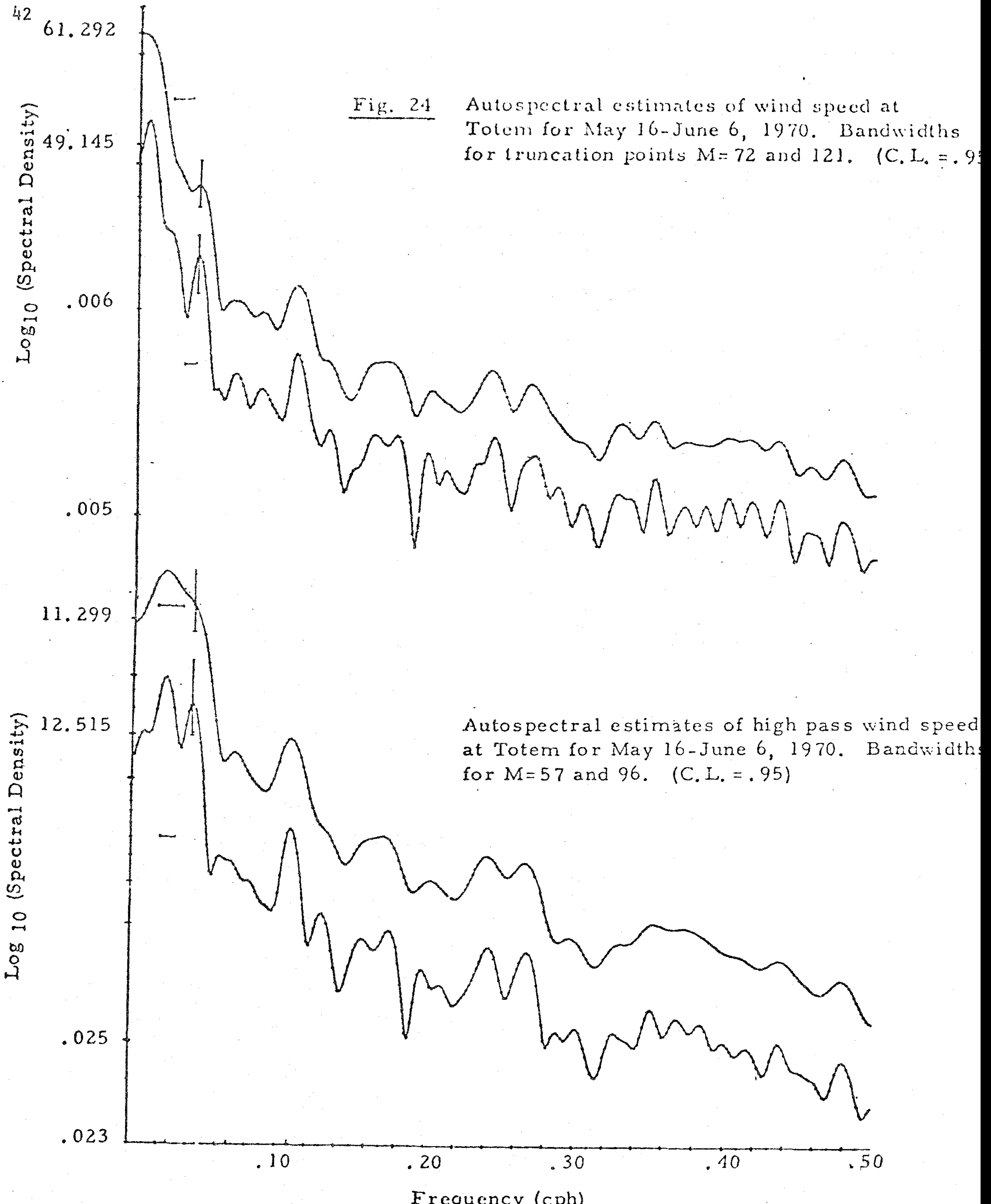

Fig. 24 Autospectral estimates of wind speed at Totem for May 16-June 6, 1970. Bandwidths for truncation points M= 72 and 121. (C.L. =.9

Autospectral estimates of high pass wind speed at Totem for May 16-June 6, 1970. Bandwidths for M=57 and 96. (C.L.=.95)

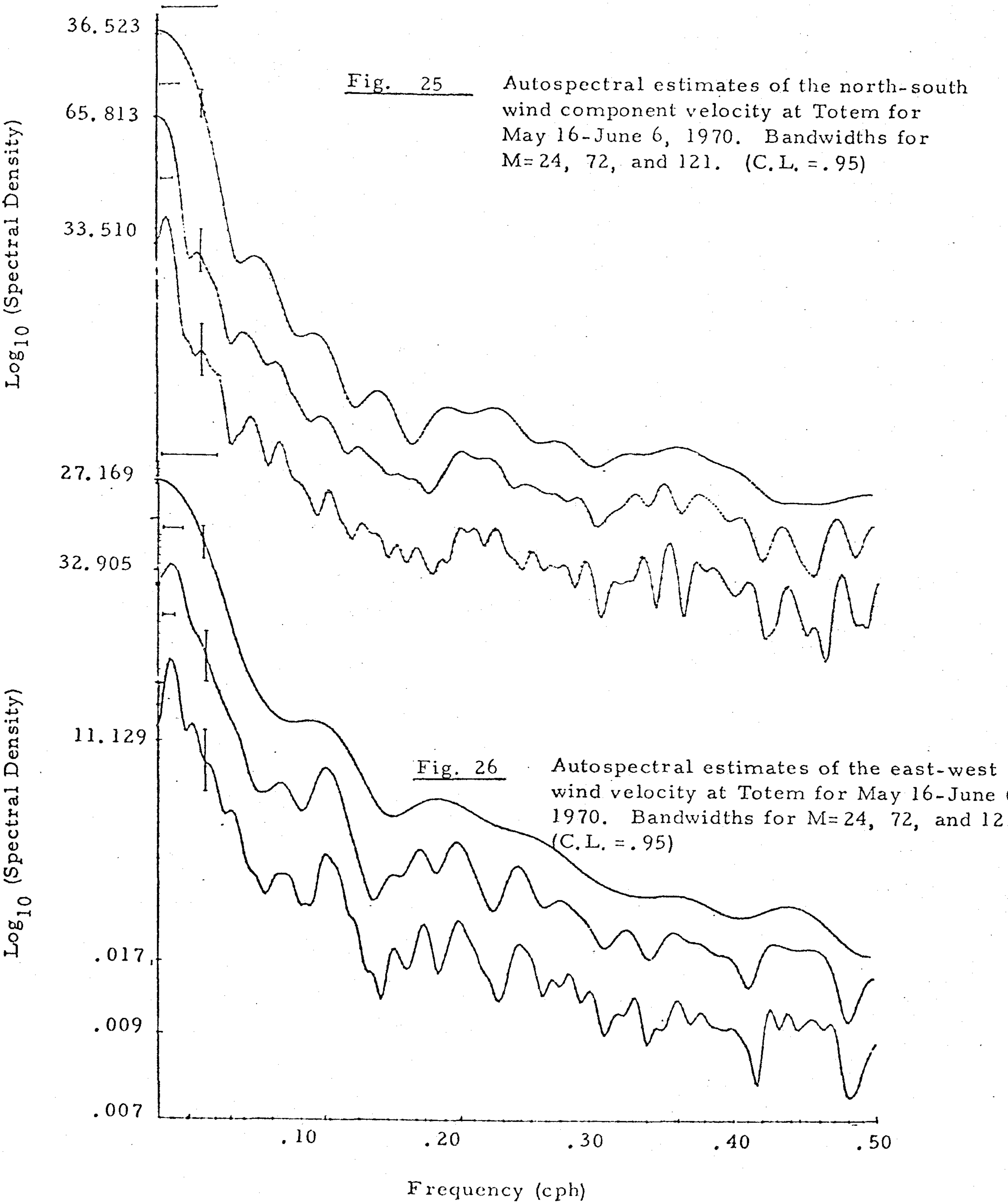

Fig. 25 Autospectral estimates of the north-south wind component velocity at Totem for May 16-June 6, 1970. Bandwidths for M=24, 72, and 121. (C.L. =.95)

Fig. 26 Autospectral estimates of the east-west wind velocity at Totem for May 16-June 6 1970. Bandwidths for M=24, 72, and 121 (C.L. =.95)

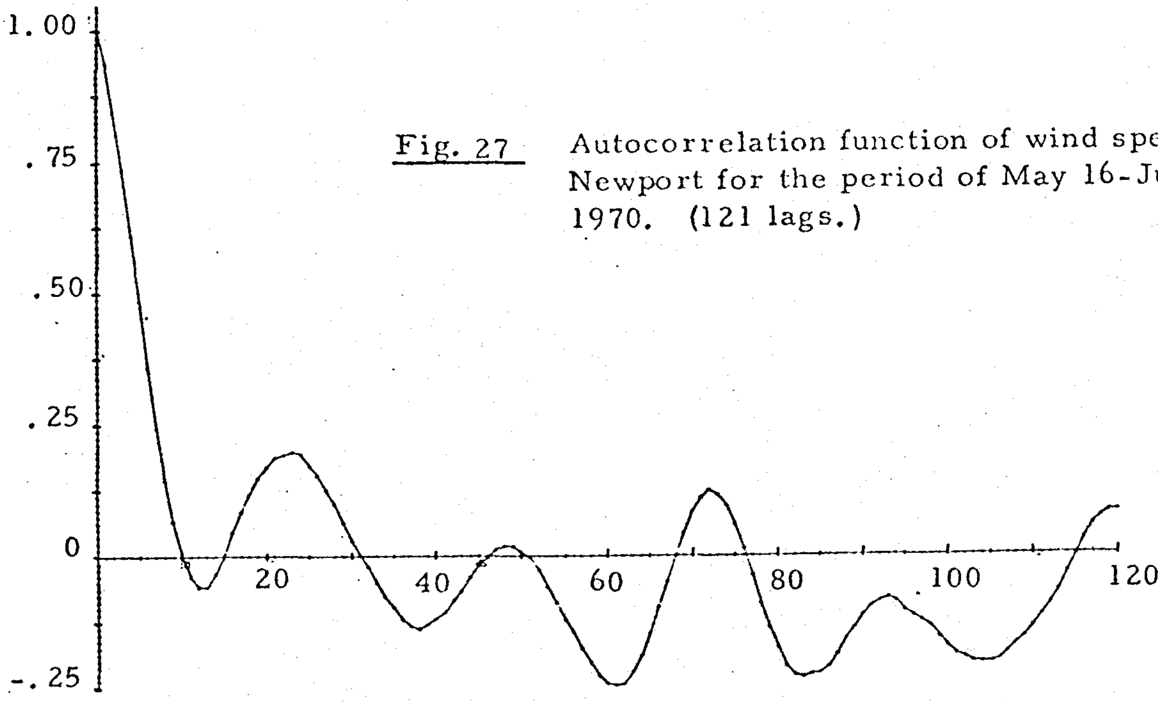

Fig. 27 Autocorrelation function of wind speed at Newport for the period of May 16-June 6, 1970. (121 lags.)

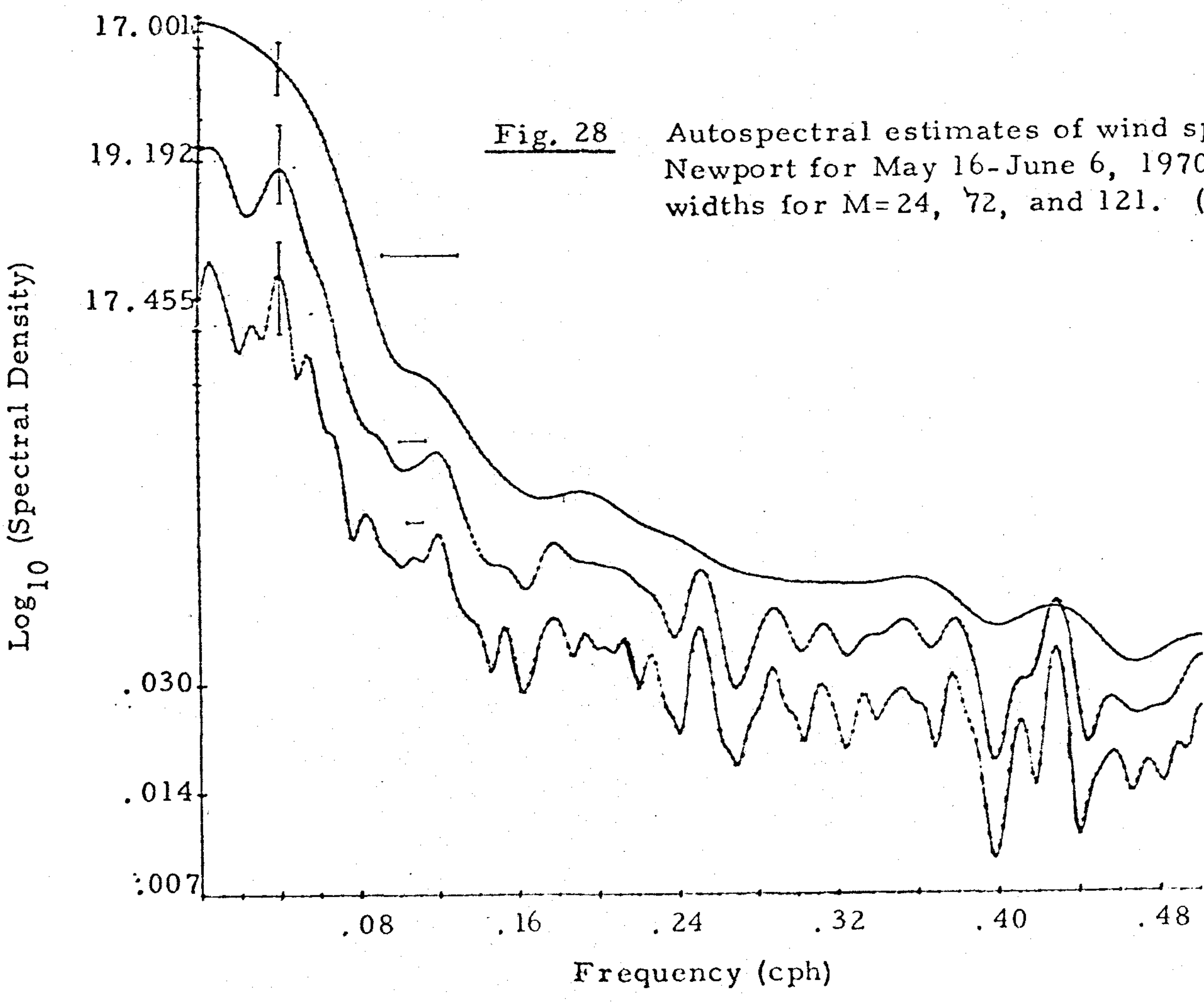

Fig. 28 Autospectral estimates of wind speed at Newport for May 16-June 6, 1970. Bandwidths for M=24, 72, and 121. (C.L. =.95)

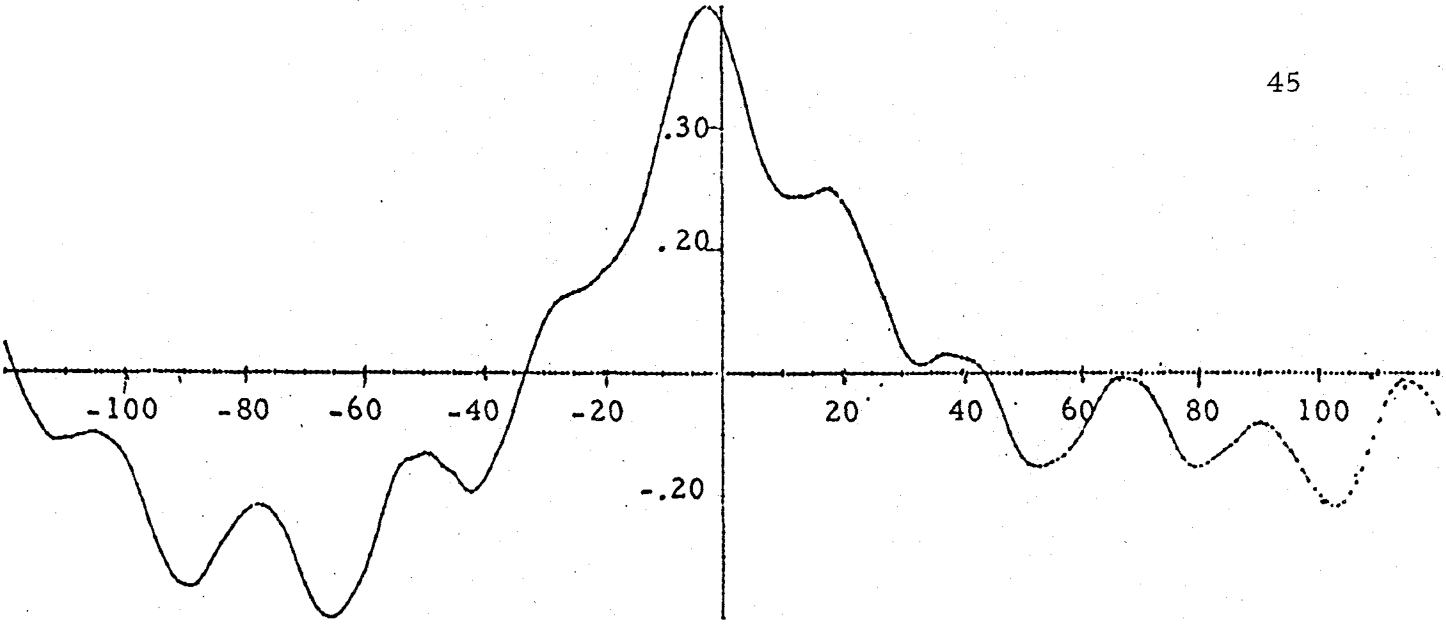

Fig. 29a. Crosscorrelation function of Totem-Newport wind speeds for March 16-June6, 1970. (121 lags.)

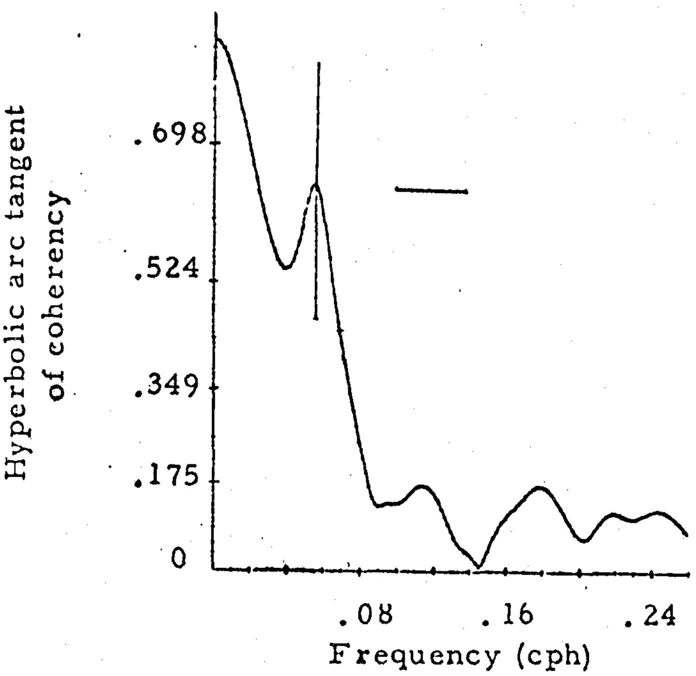

Fig. 29b. Coherency estimates of Totem-Newport wind speeds for March 16-June 6, 1970. Bandwidth for M=24. (C. L. = .95)

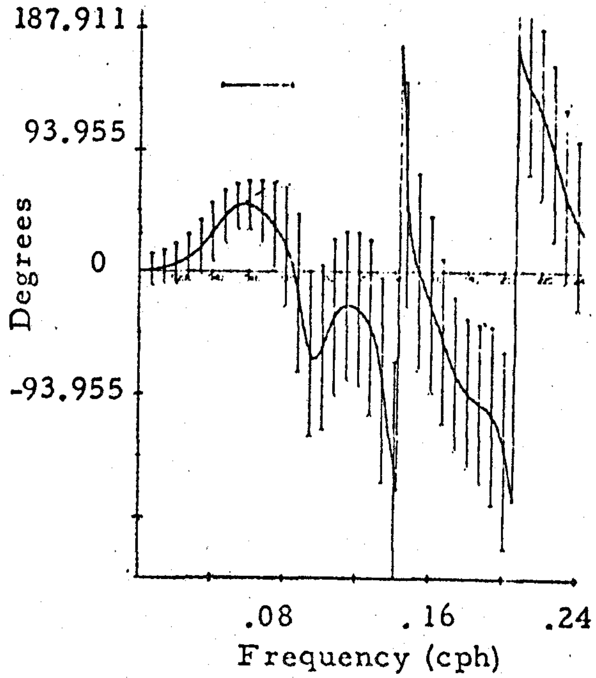

Fig. 29c. Phase estimates of Totem-Newport wind speeds for May 16-June 6, 1970. Bandwidth for M=24. (C. L. = .95)

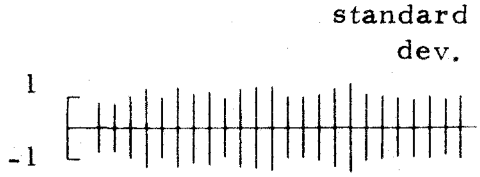

Fig. 30(a) Wind Speed

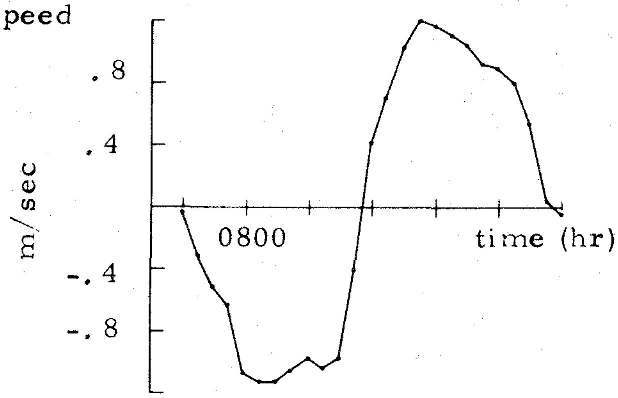

Fig. 30(b) North-South
(V) Velocity
Component

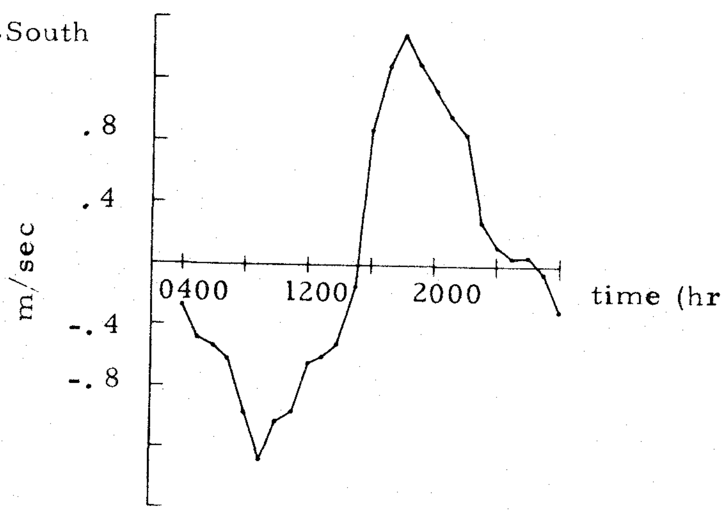

Fig. 30(c) East-West
(U) Velocity
Component

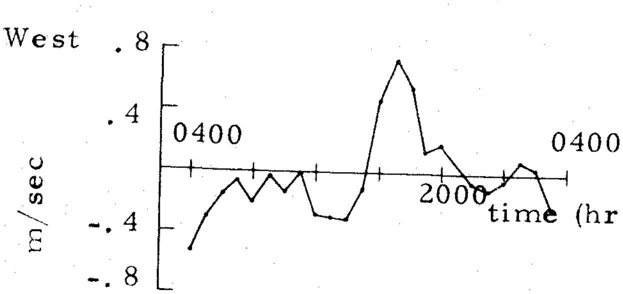

Fig. 30 (a) - (c) Average diurnally varying portion of wind speed, U and V Velocity components at Totem for May 16 - June 6, 1970.

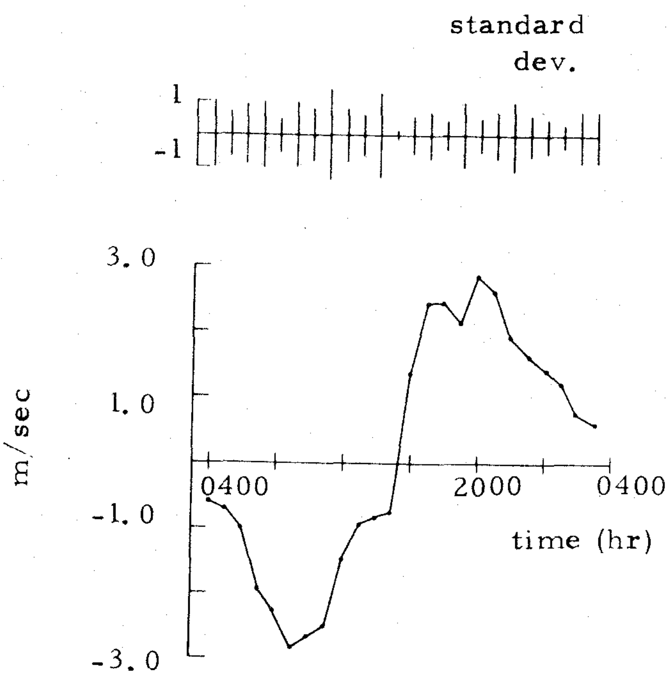

Fig. 30(d). Hourly averages of diurnally varying wind speed selected days (17, 23, 26, 30, 31 May 1970)

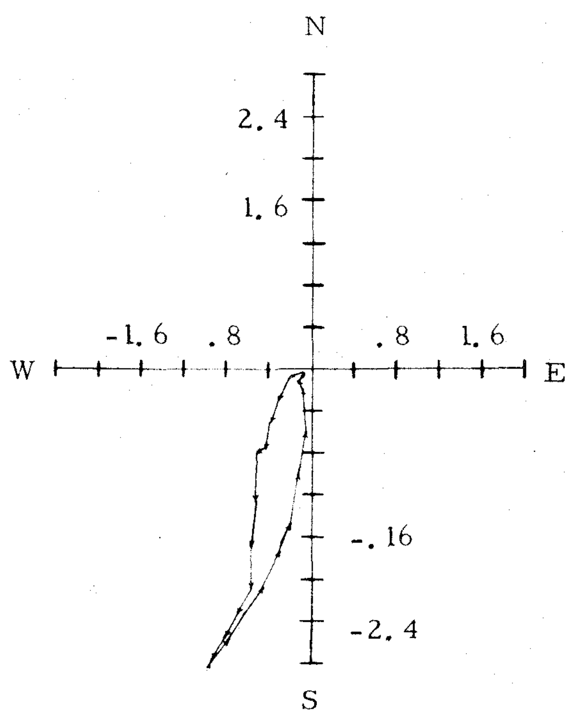

Fig. 30(e) Progressive vector diagram of average diurnally varying portion of wind speed at Totem.

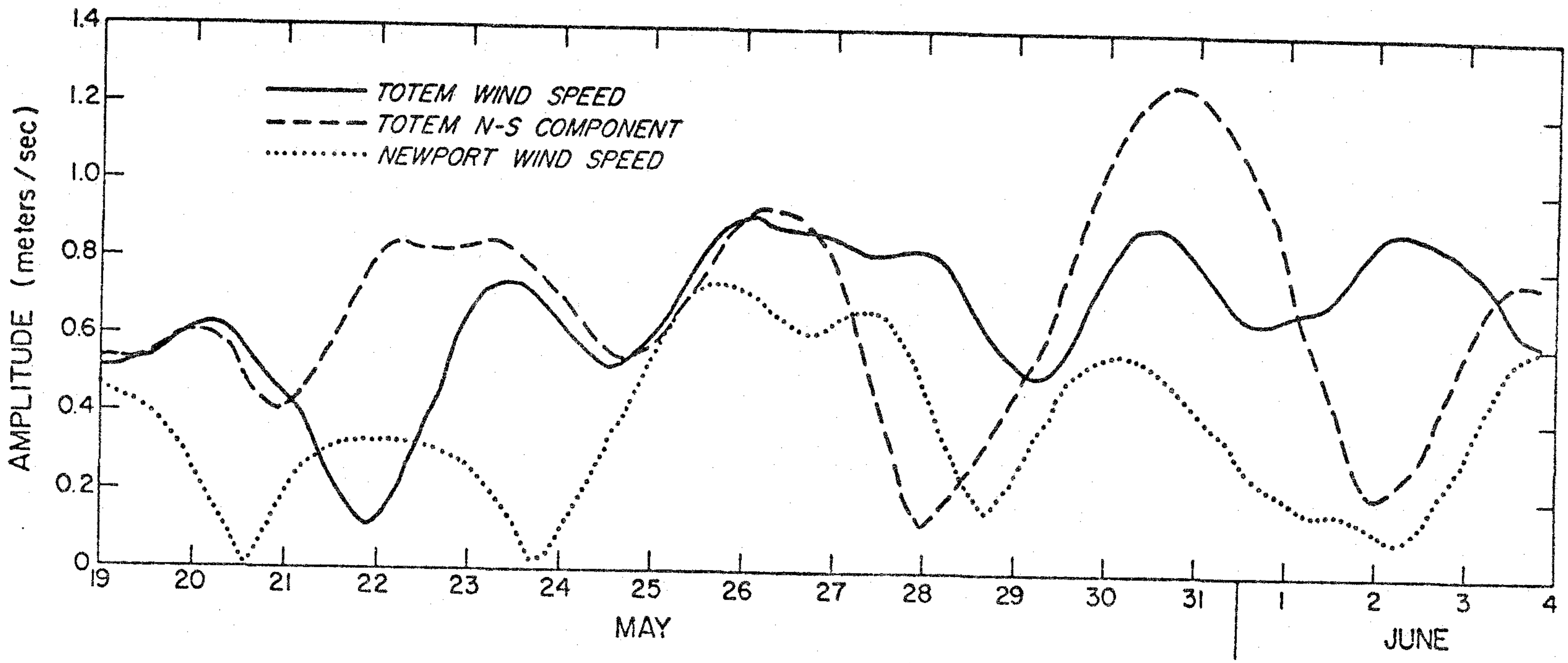

Fig. 31. Complex demodulates at 24 hour period of wind speed and north-south velocity component at TOTEM, and of wind speed at Newport, for May 16 - June 6, 1970

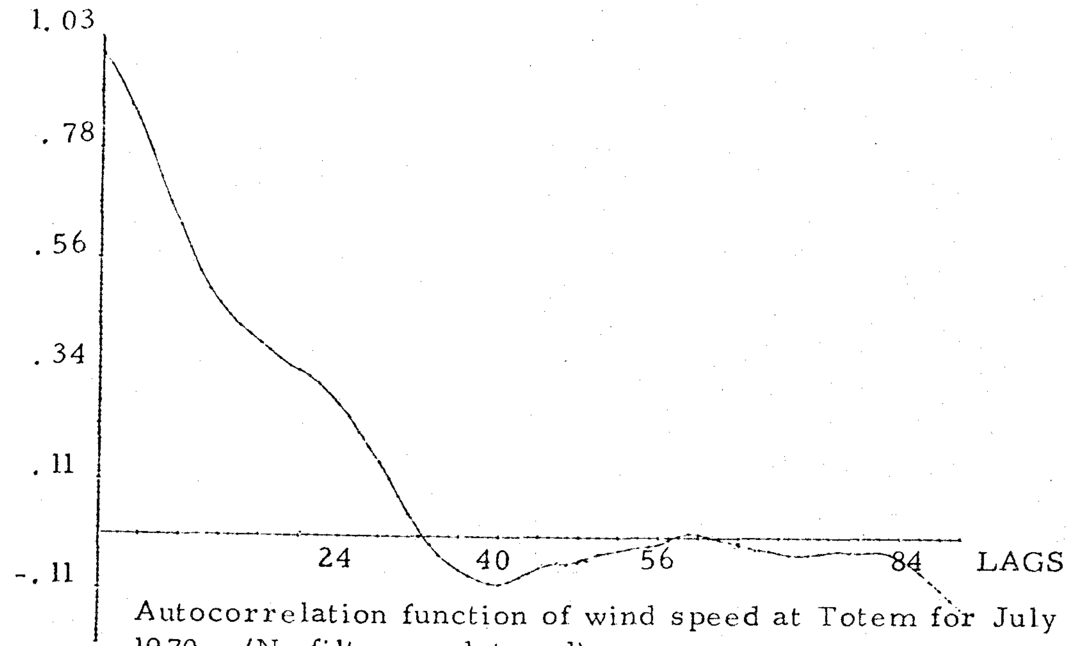

Autocorrelation function of wind speed at Totem for July 1970. (No filter or detrend)

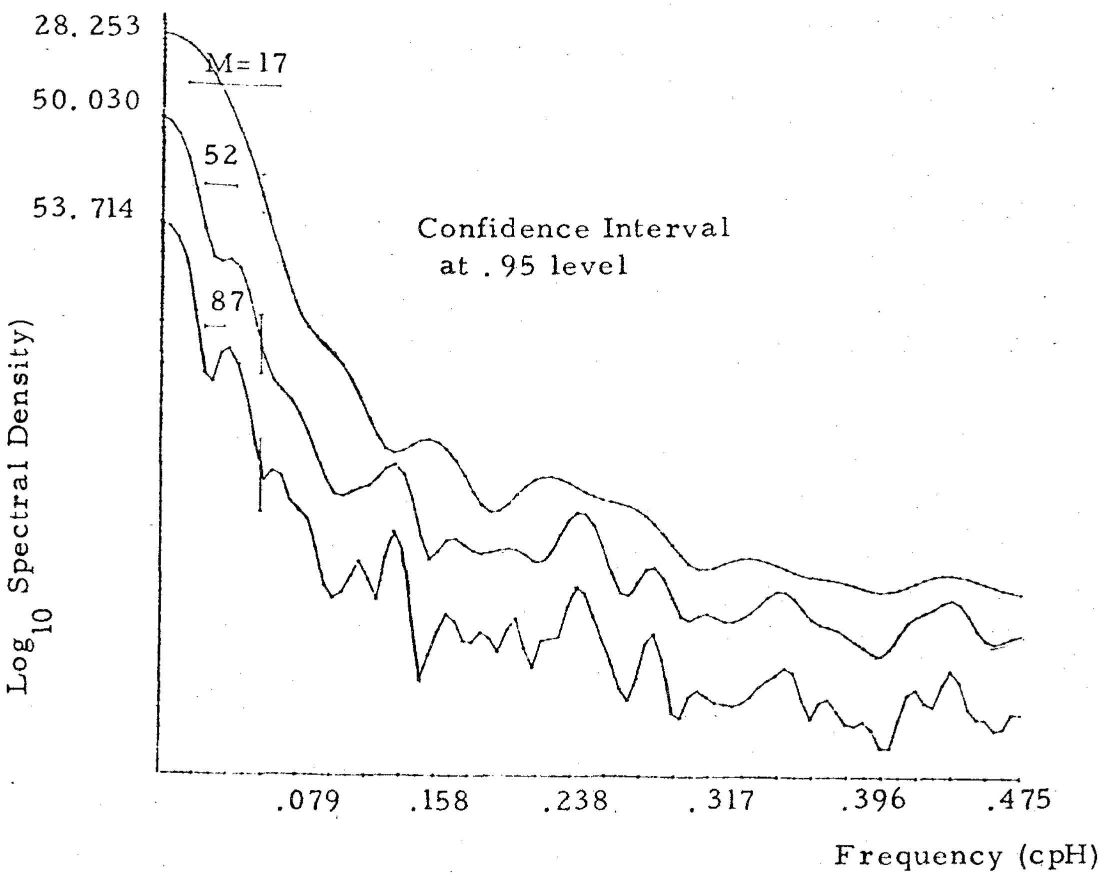

Fig. 32. Power spectra of wind speed at Totem for July, 1970. Bandwidths for M=17, 52 and 87. (No filter or detrend)

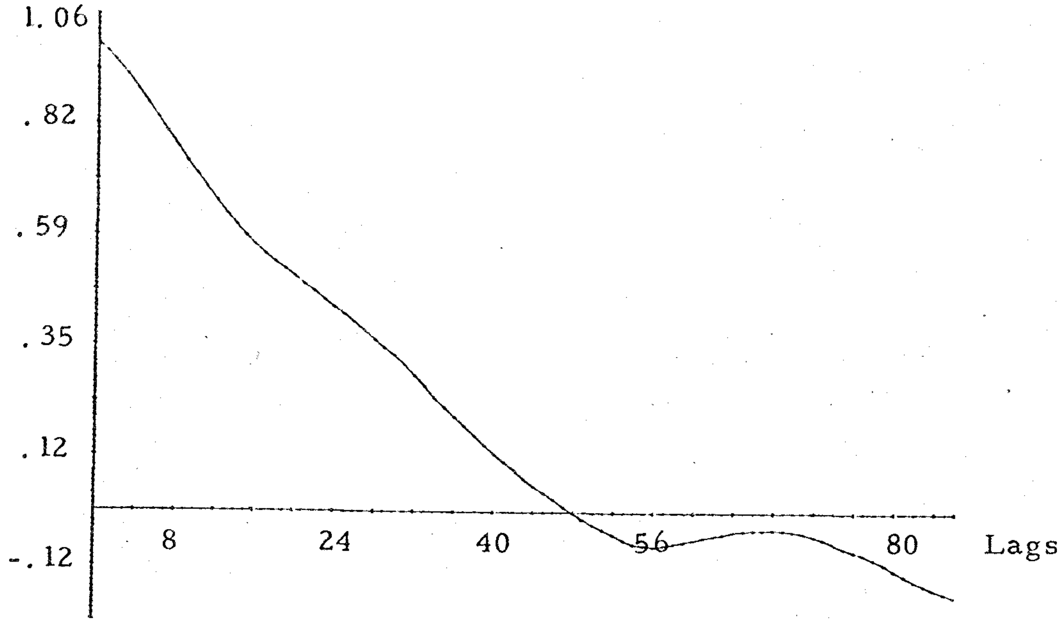

Autocorrelation function of wind U component at Totem for July, 1970 (No filter or detrend)

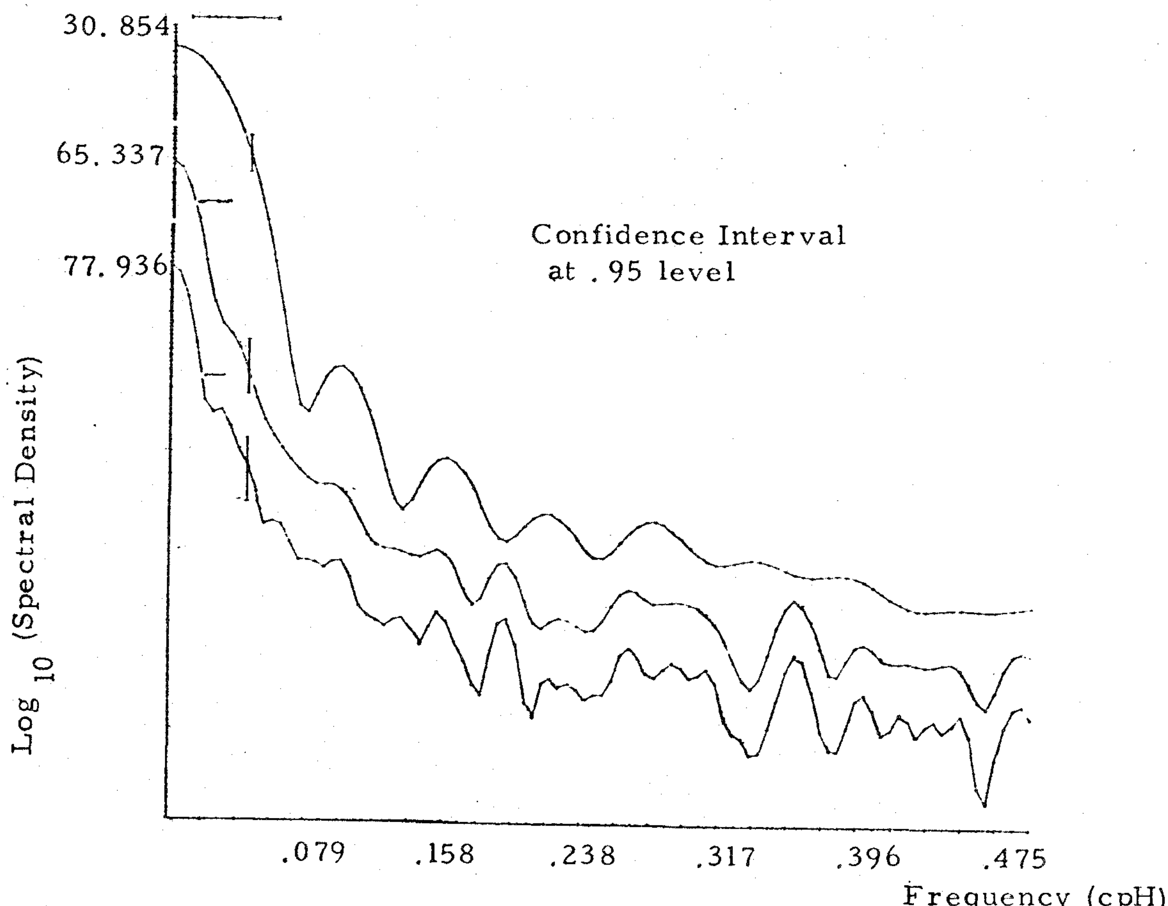

Fig. 33. Power spectra of wind U component at Totem for July 1970. Bandwidths for M= 17, 52 and 87. (No filter or detrend)

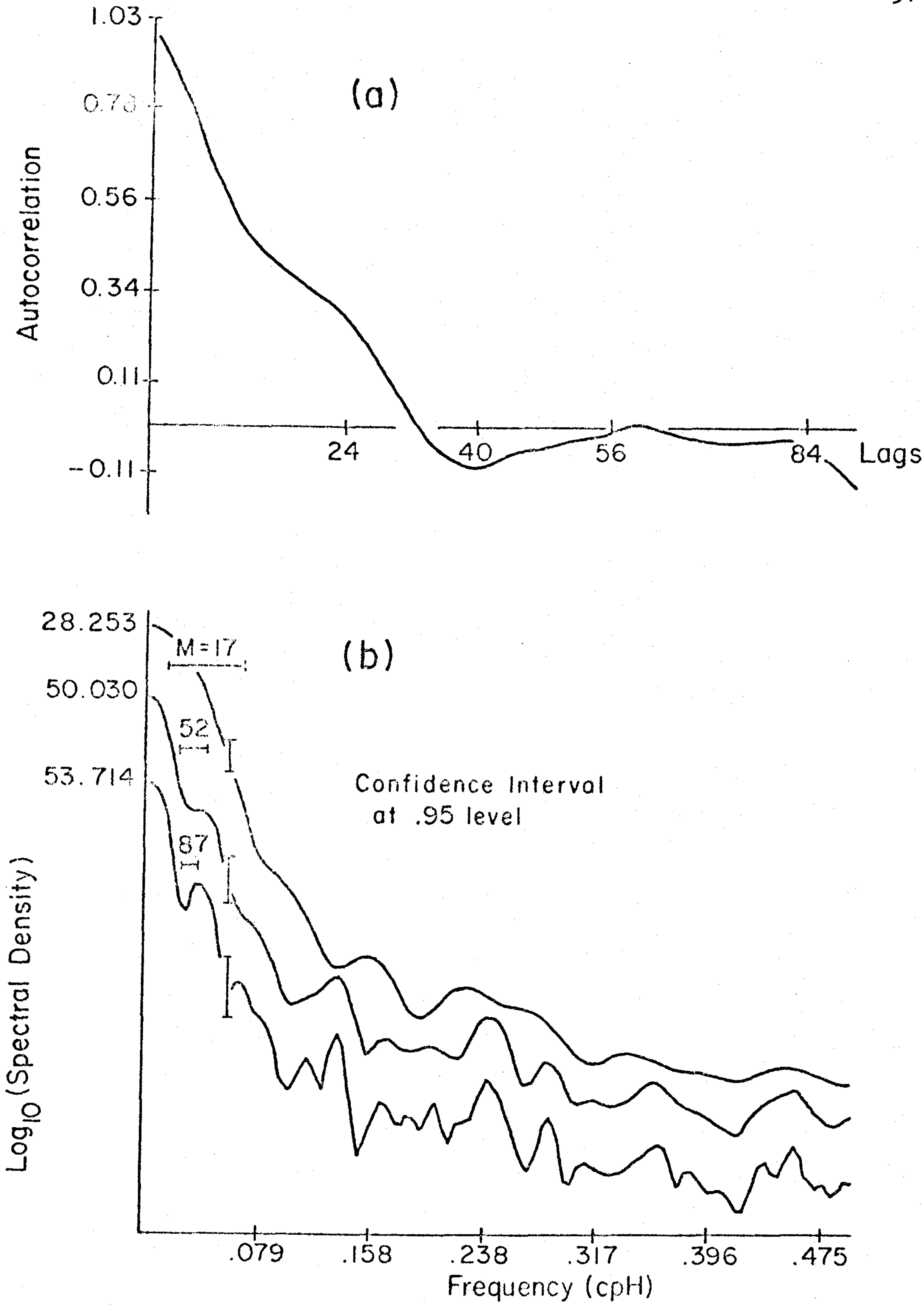

Figure 34. Power spectra of wind V component at Totem for July, 1970, Bandwidths for M = 17, 52 and 87. (No filter or detrend)

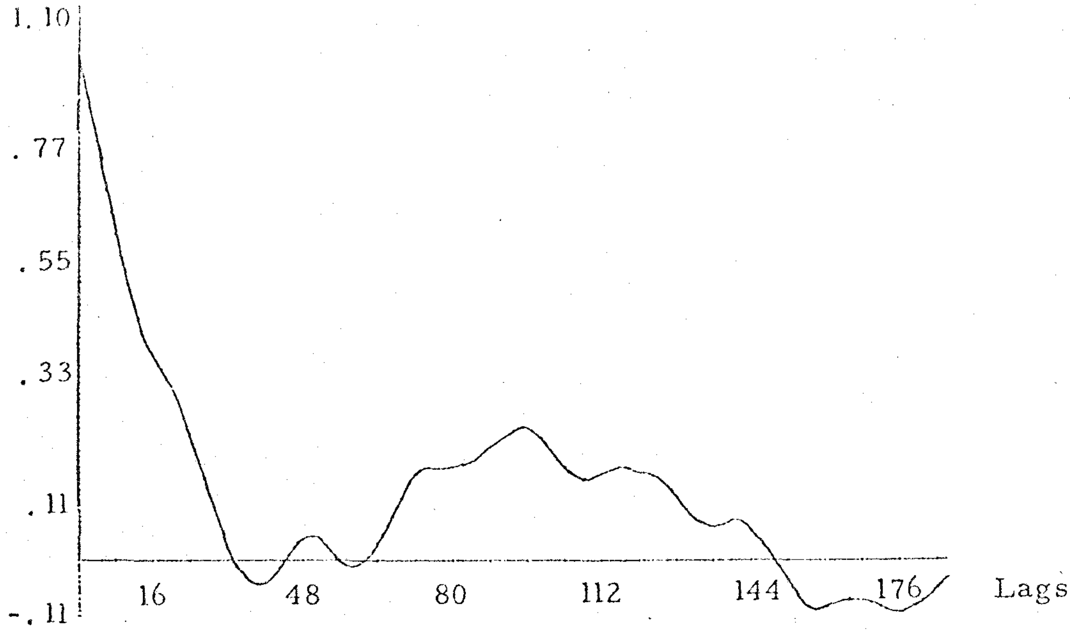

Autocorrelation function of wind speed at Totem for August, 1970. (No filter or detrend).

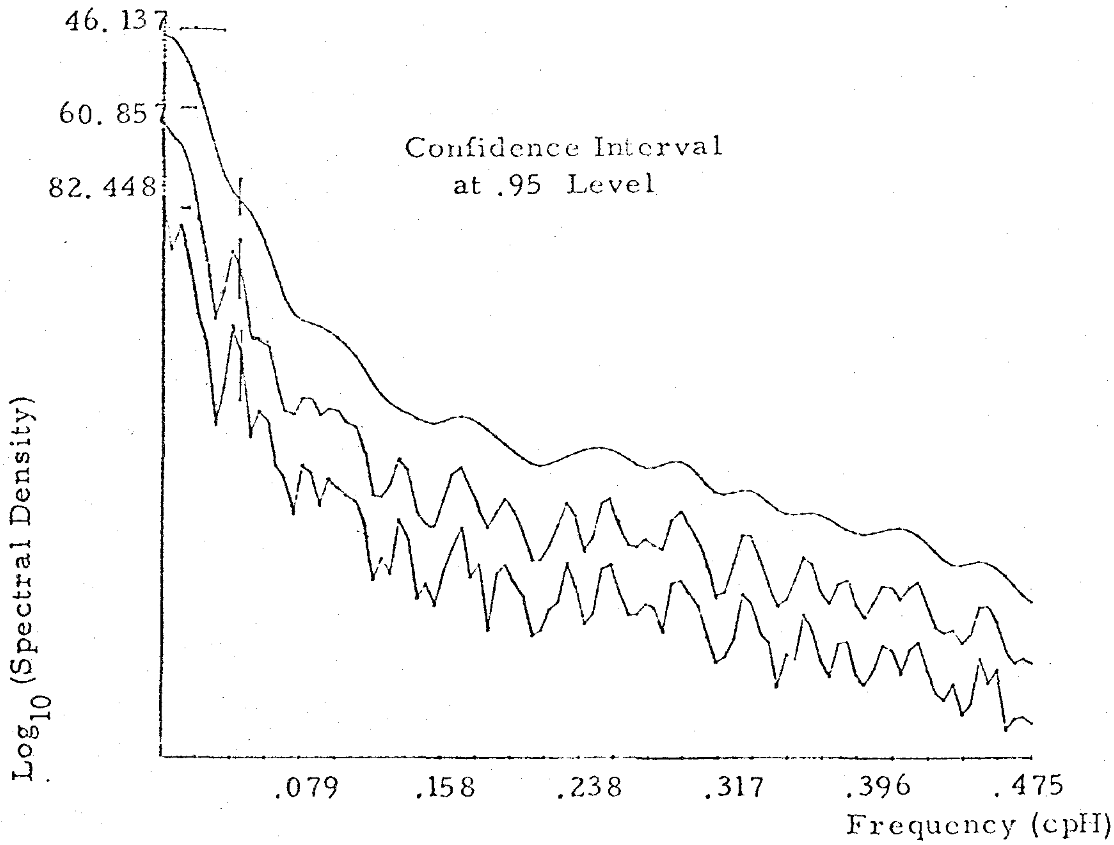

Fig. 35. Power spectra of wind speed at Totem for August, 1970. Bandwidths for M=37, 112 and 187. (No filter or detrend).

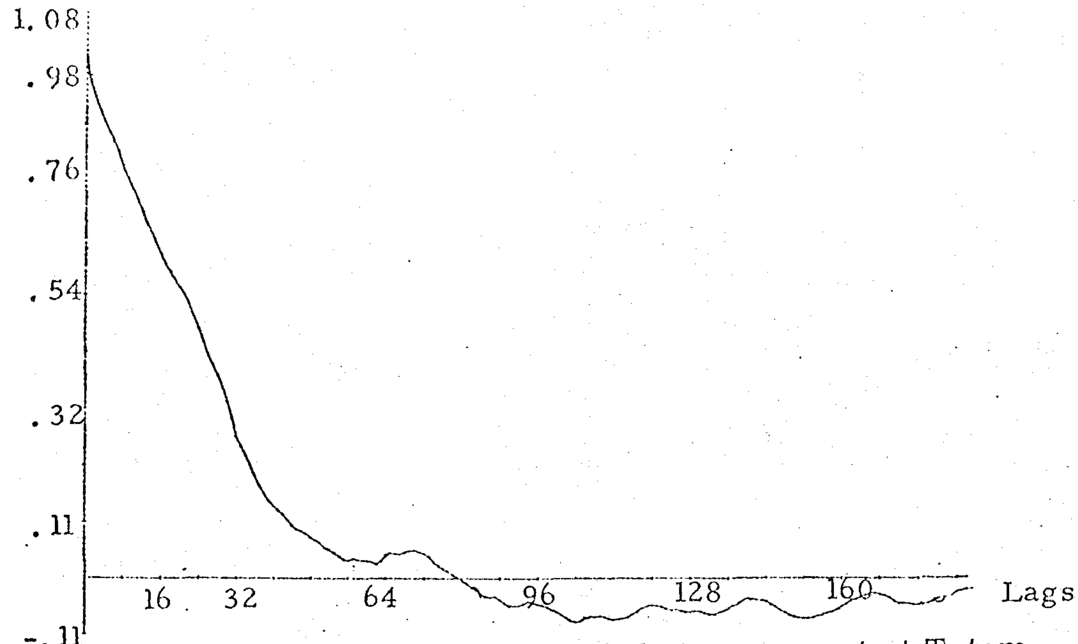

Autocorrelation function of wind U component at Totem for August, 1970. (No filter or detrend)

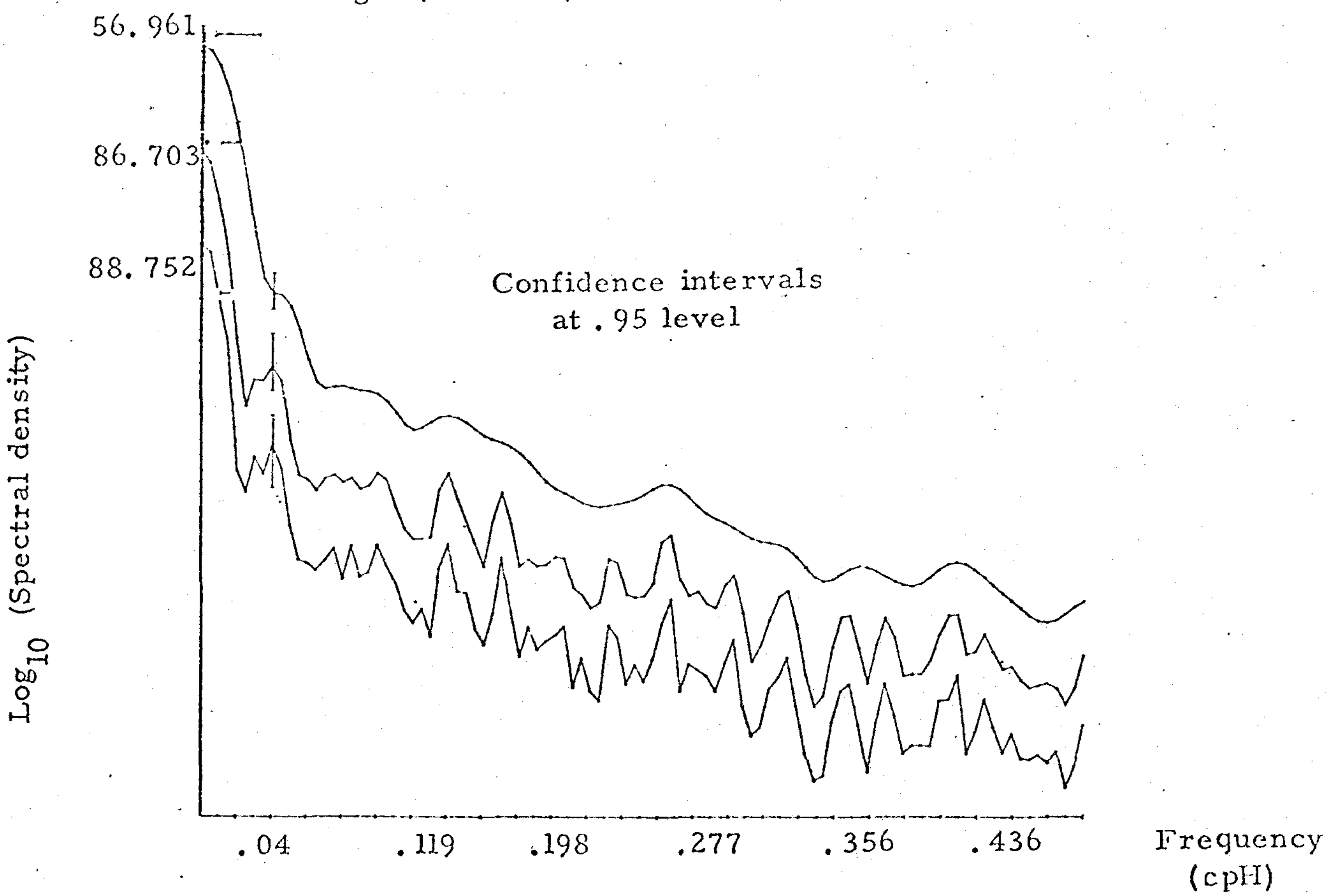

Fig. 36. Power spectra of wind U component at Totem for August, 1970. Bandwidths for M=37, 112 and 187. (no filter or detrend)

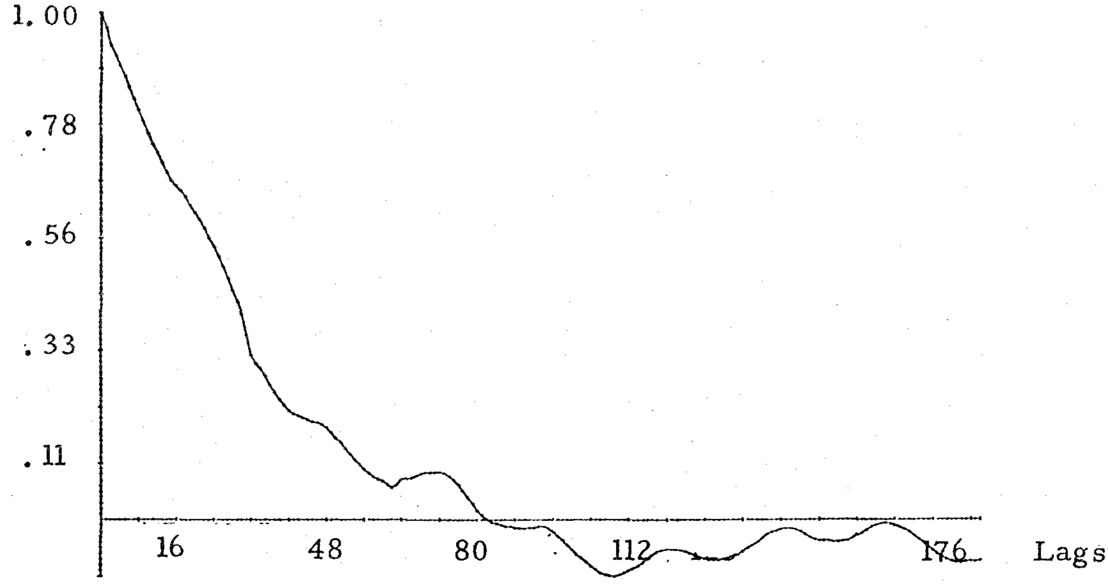

Autocorrelation function of wind V component at Totem for August, 1970. (No filter or detrend)

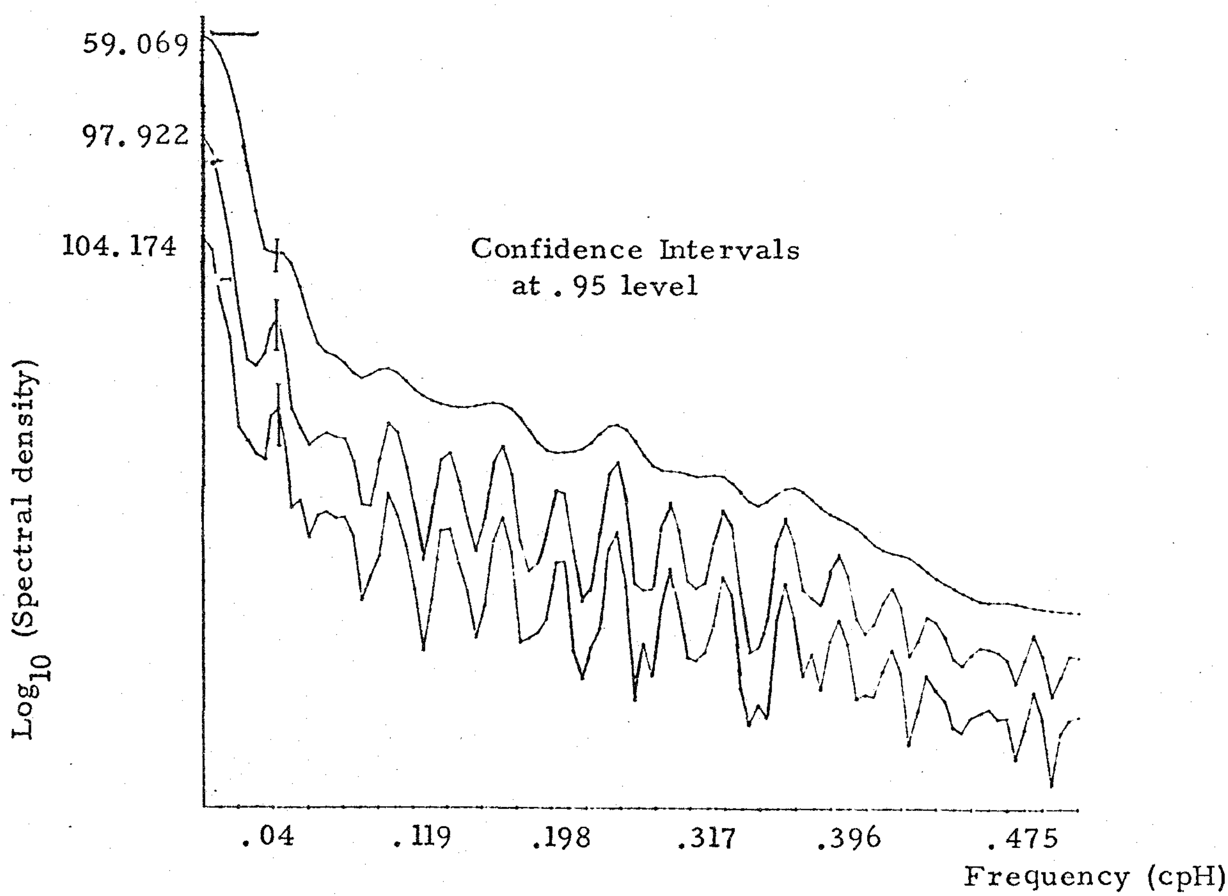

Fig. 37. Power spectra of wind V component at Totem for August, 1970. Bandwidths for m=37, 112 and 137 (no filter or detrend)

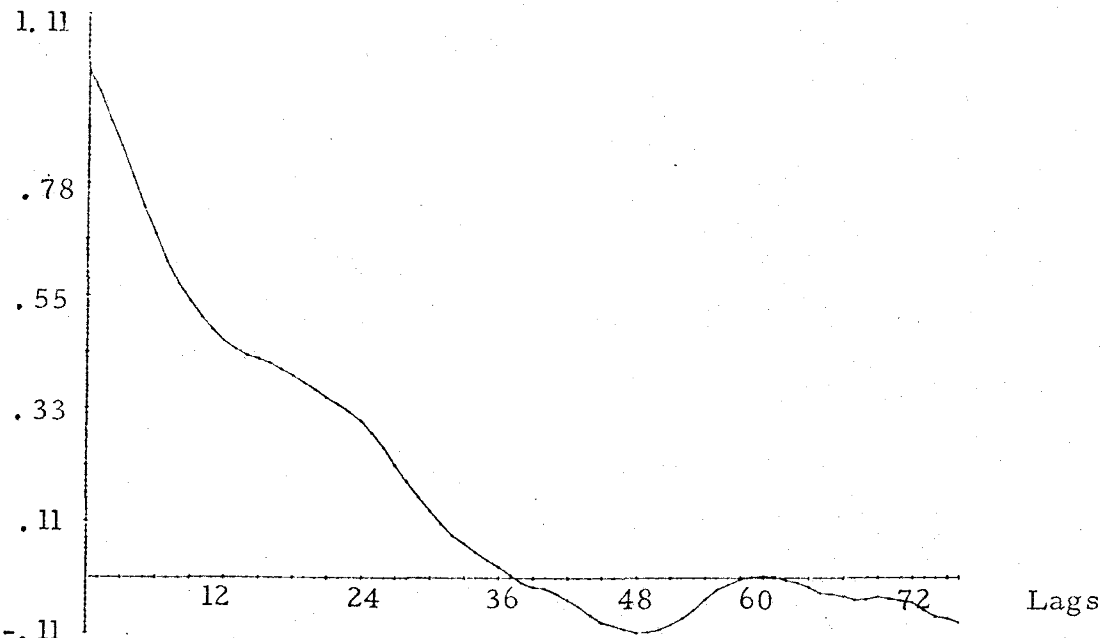

Autocorrelation function of wind speed at Totem for September, 1970 (No filter or detrend)

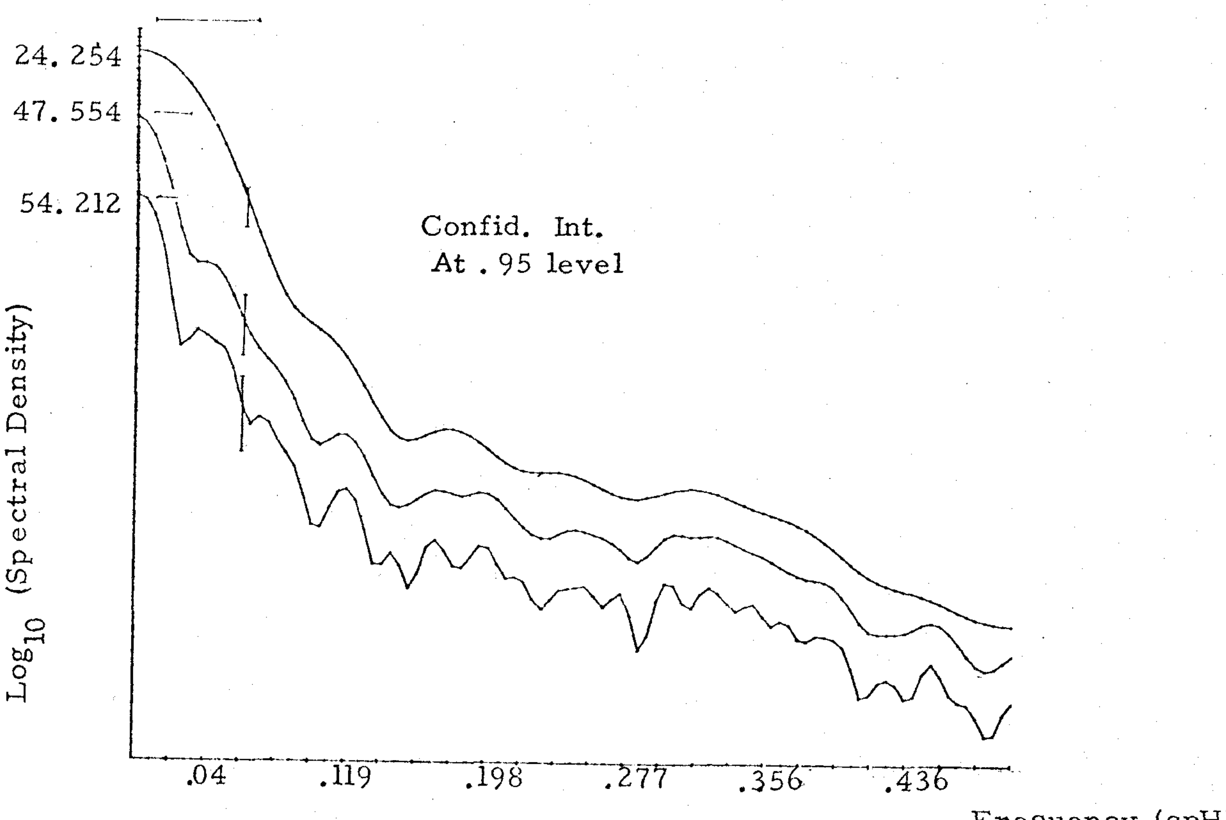

Fig. 38. Power spectra of wind speed at Totem for September, 1970. Bandwidths for M=15, 46, and 77. (No filter or detrend)

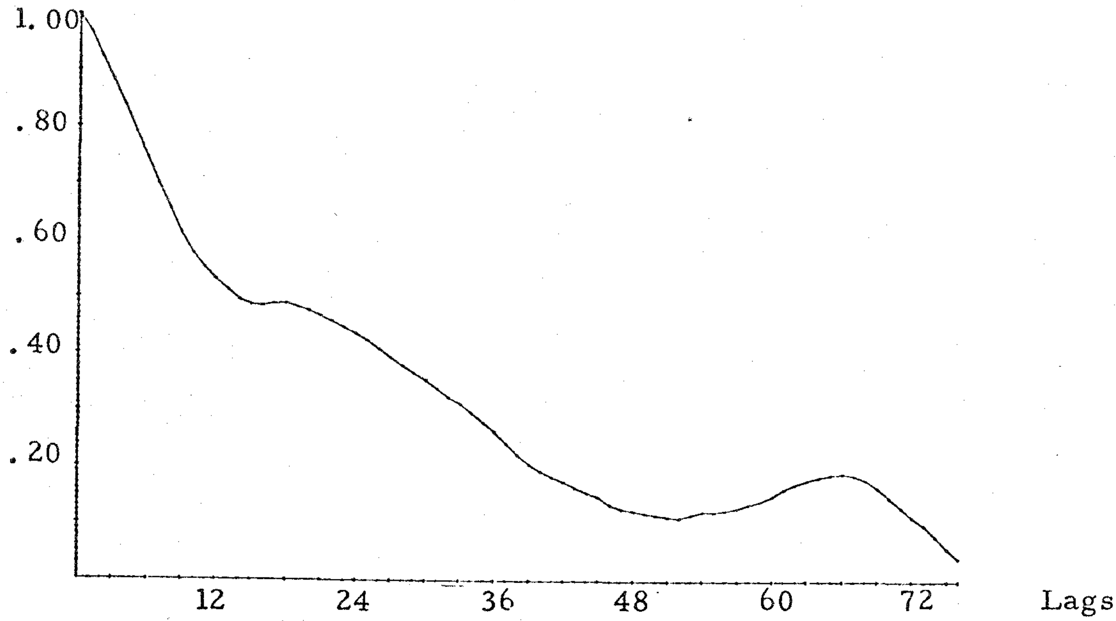

Autocorrelation function of wind U component at Totem for September, 1970. (No filter or detrend)

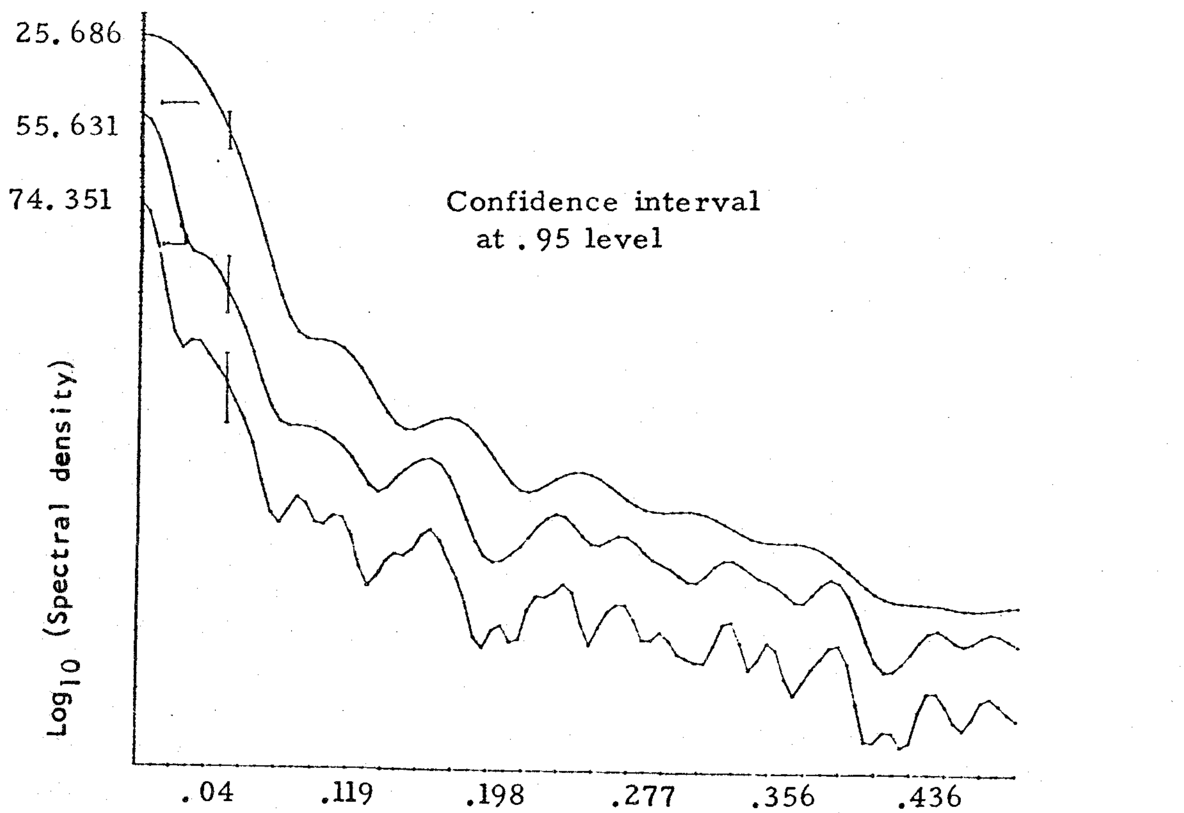

Fig. 39. Power spectra of wind U component at Totem for September, 1970. Bandwidths for M=15, 46 and 77. (No filter or detrend)

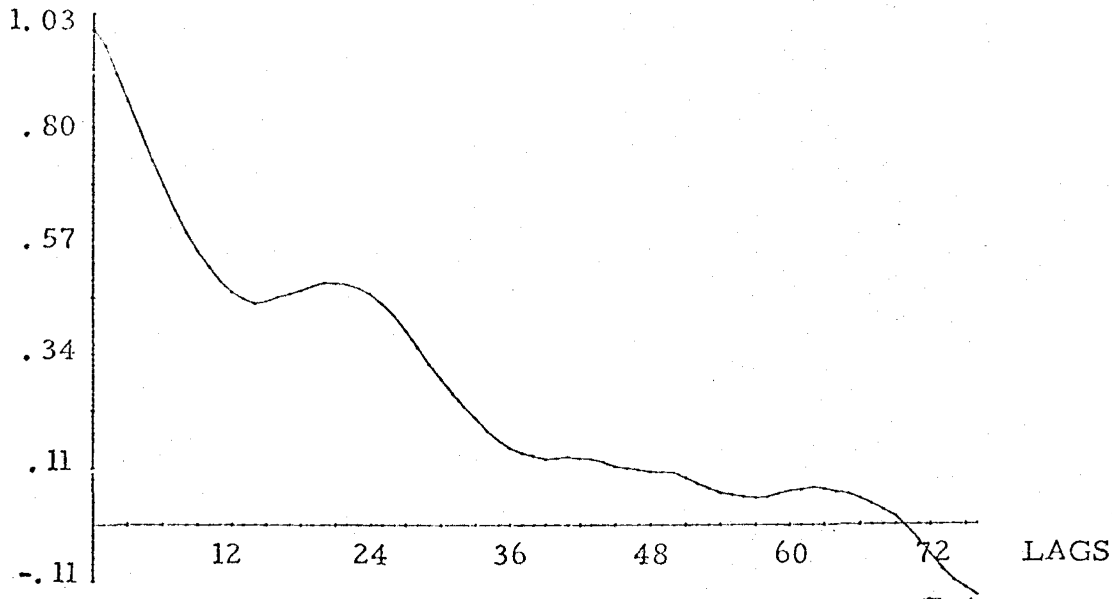

Autocorrelation function of wind V component at Totem for September, 1970. (No filter or detrend).

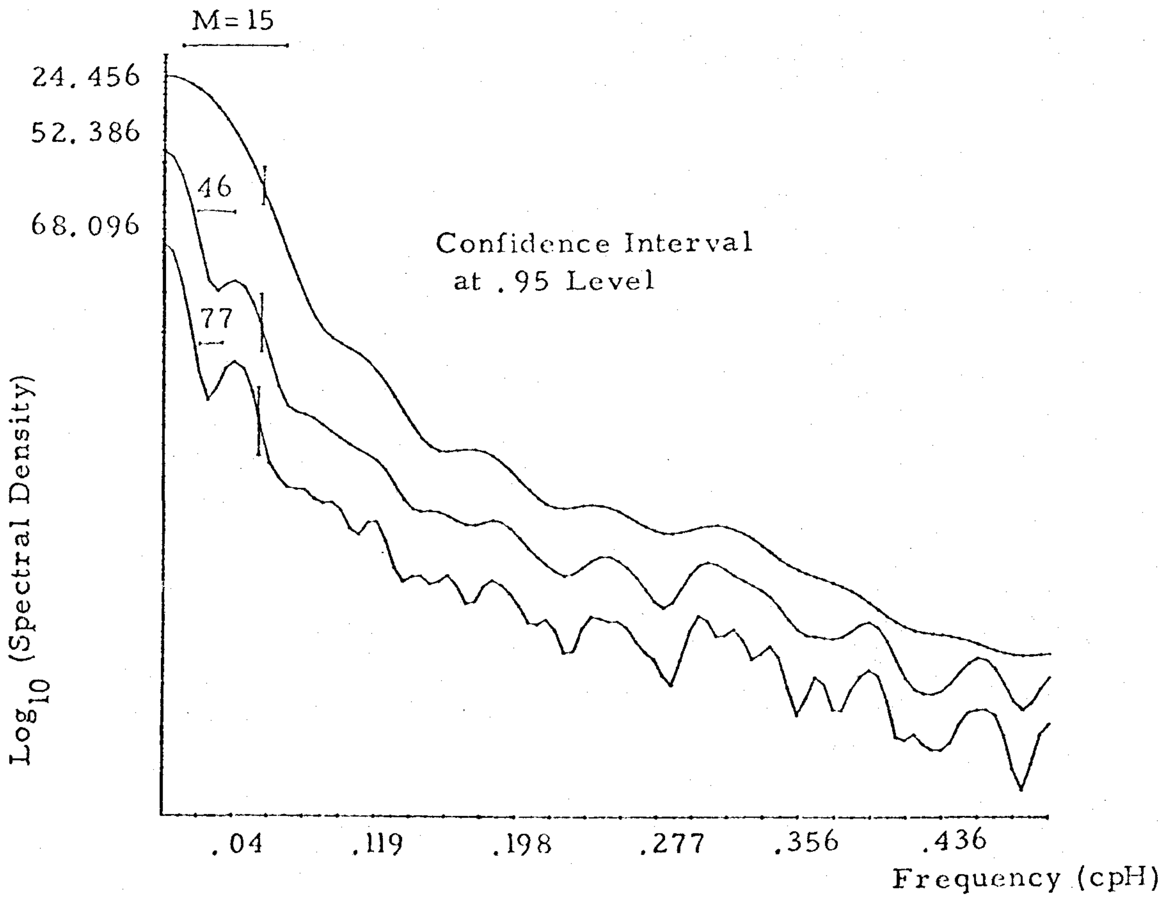

Fig. 40. Power spectra of wind V component at Totem for September, 1970. Bandwidths for M = 15, 46 and 77. (No filter of detrend)

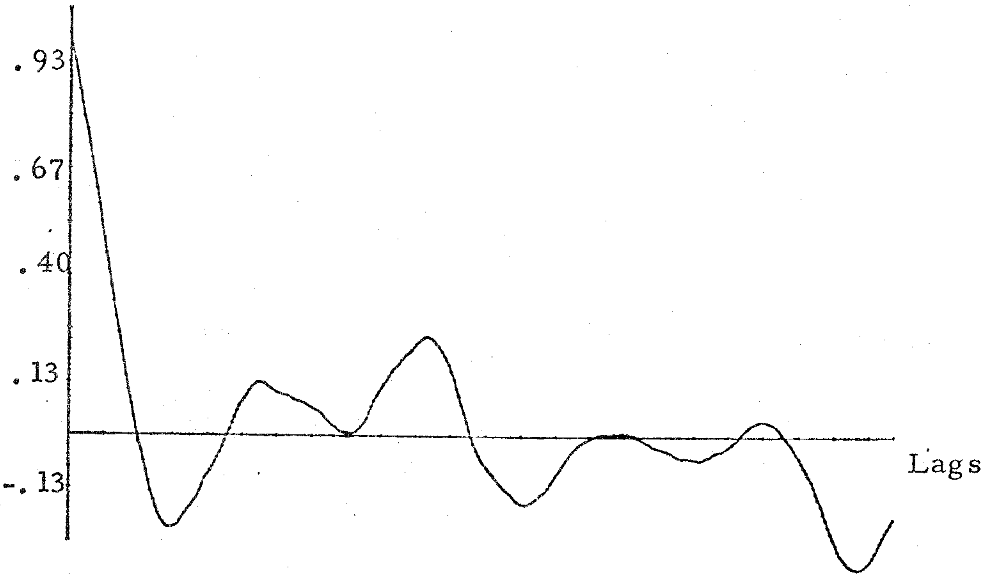

Autocorrelation function of current speed at Totem for August 5-14, 1970

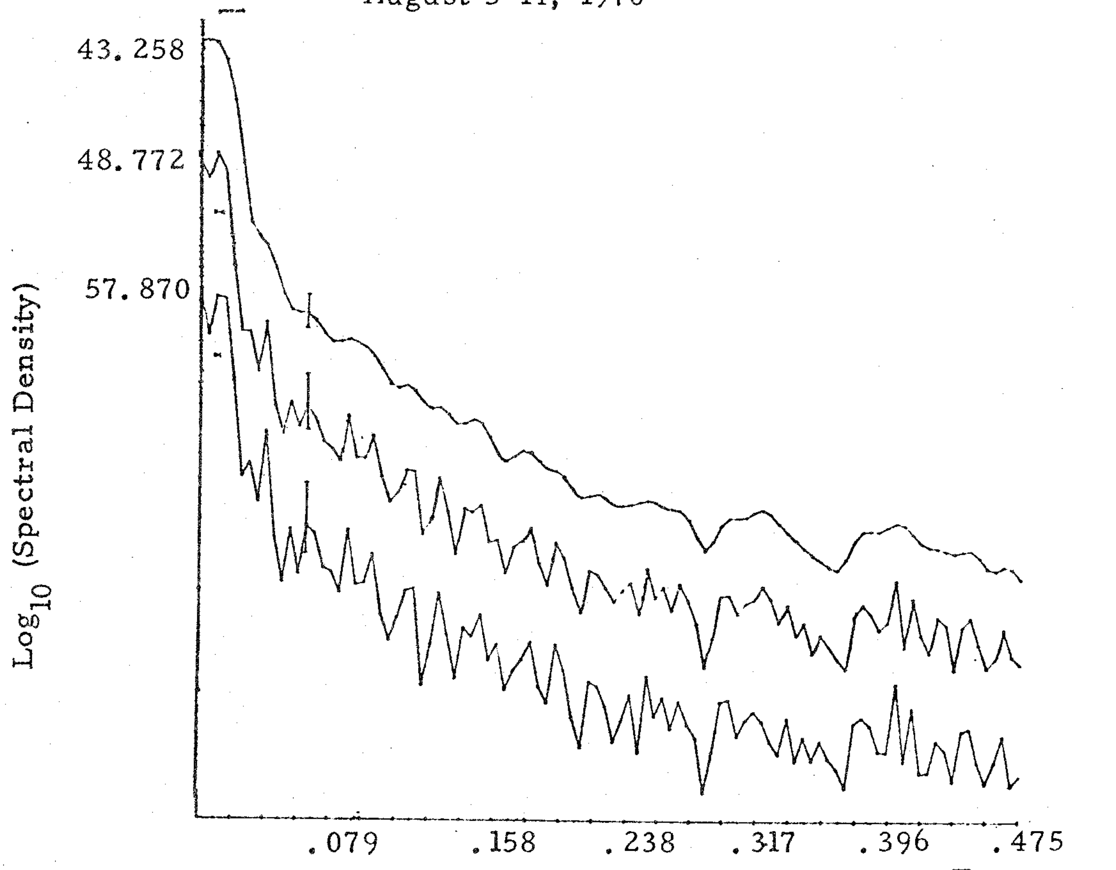

Fig. 41. Power spectra of current speed at Totem for August 5-14, 1970. Bandwidths for M=66, 199 and 333.

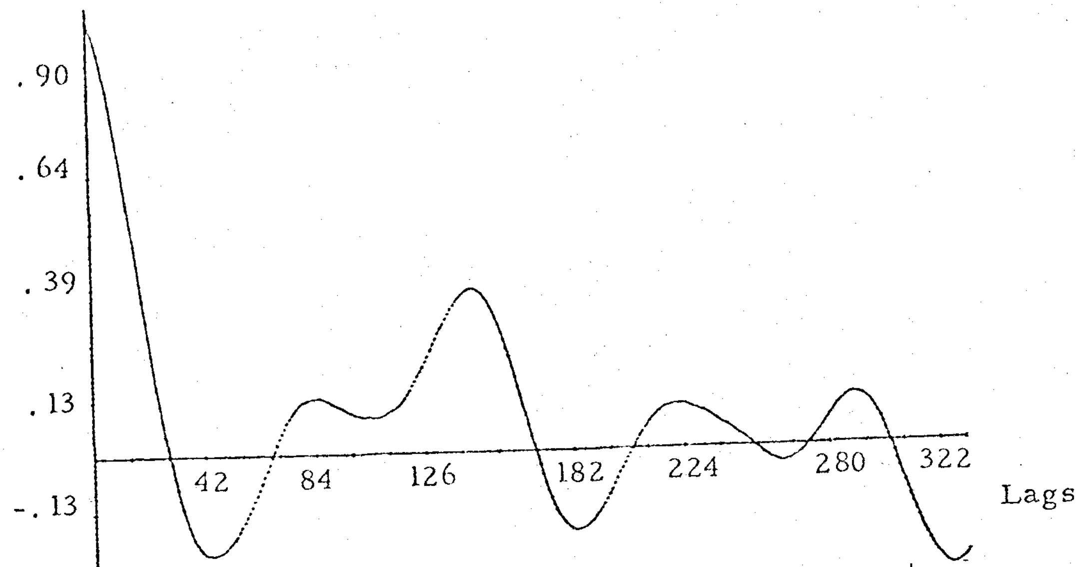

Autocorrelation function of current U component at Totem for August 5 - 14, 1970

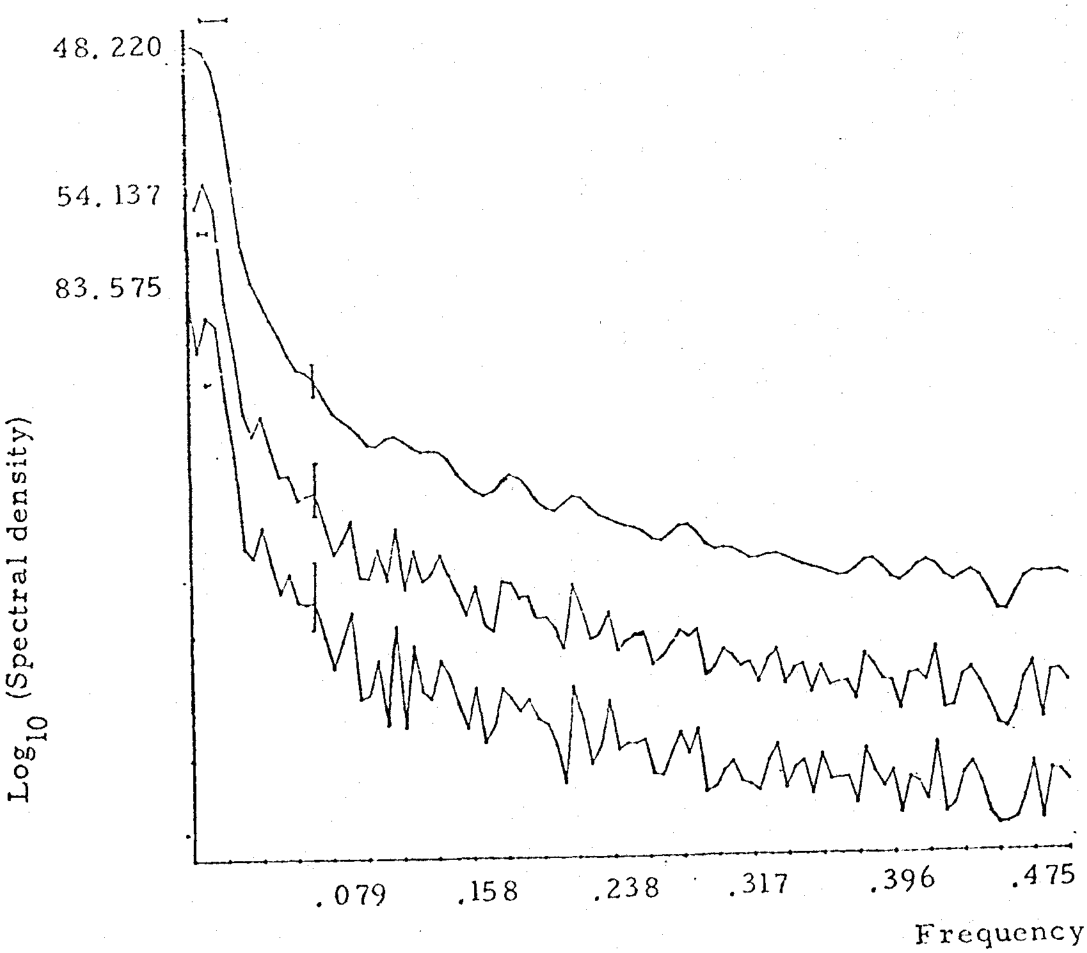

Fig. 42. Power spectra of current U component at Totem for August 5 - 14, 1970. Bandwidths for M=66, 199 and 333.

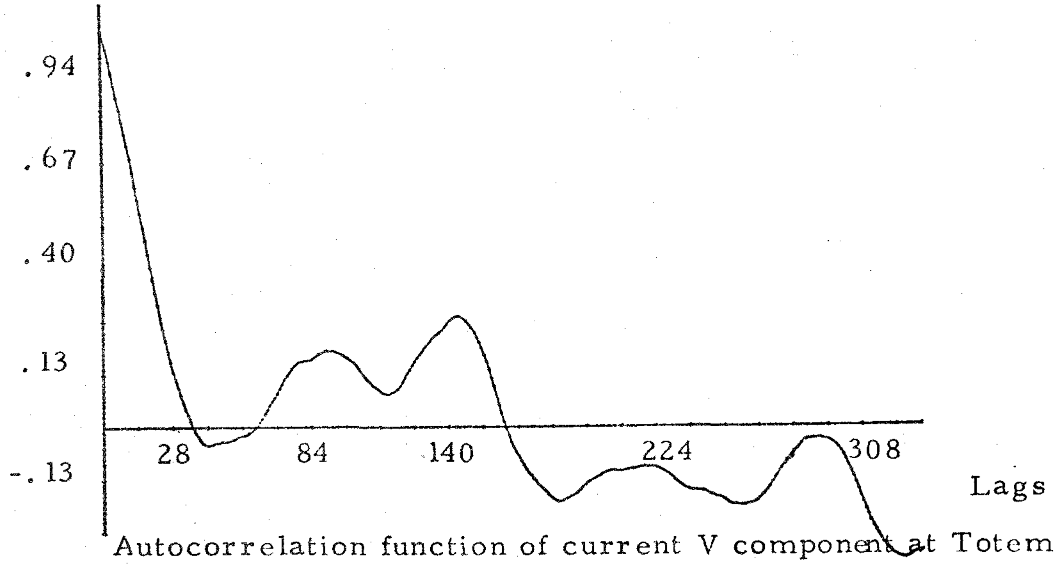

Autocorrelation function of current V component at Totem for August 5 - 14, 1970.

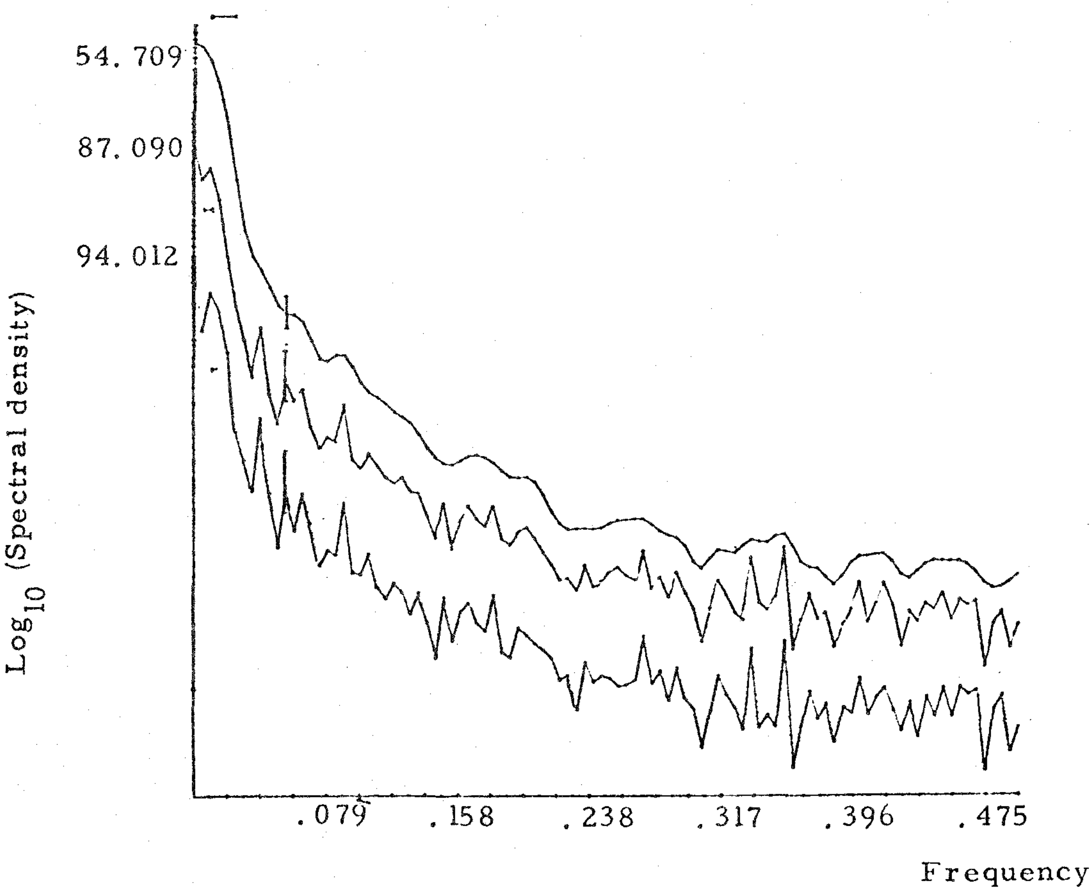

Fig. 43. Power spectra of current V component at Totem for August 5 - 14, 1970. Bandwidths for M=66, 199 and 333.

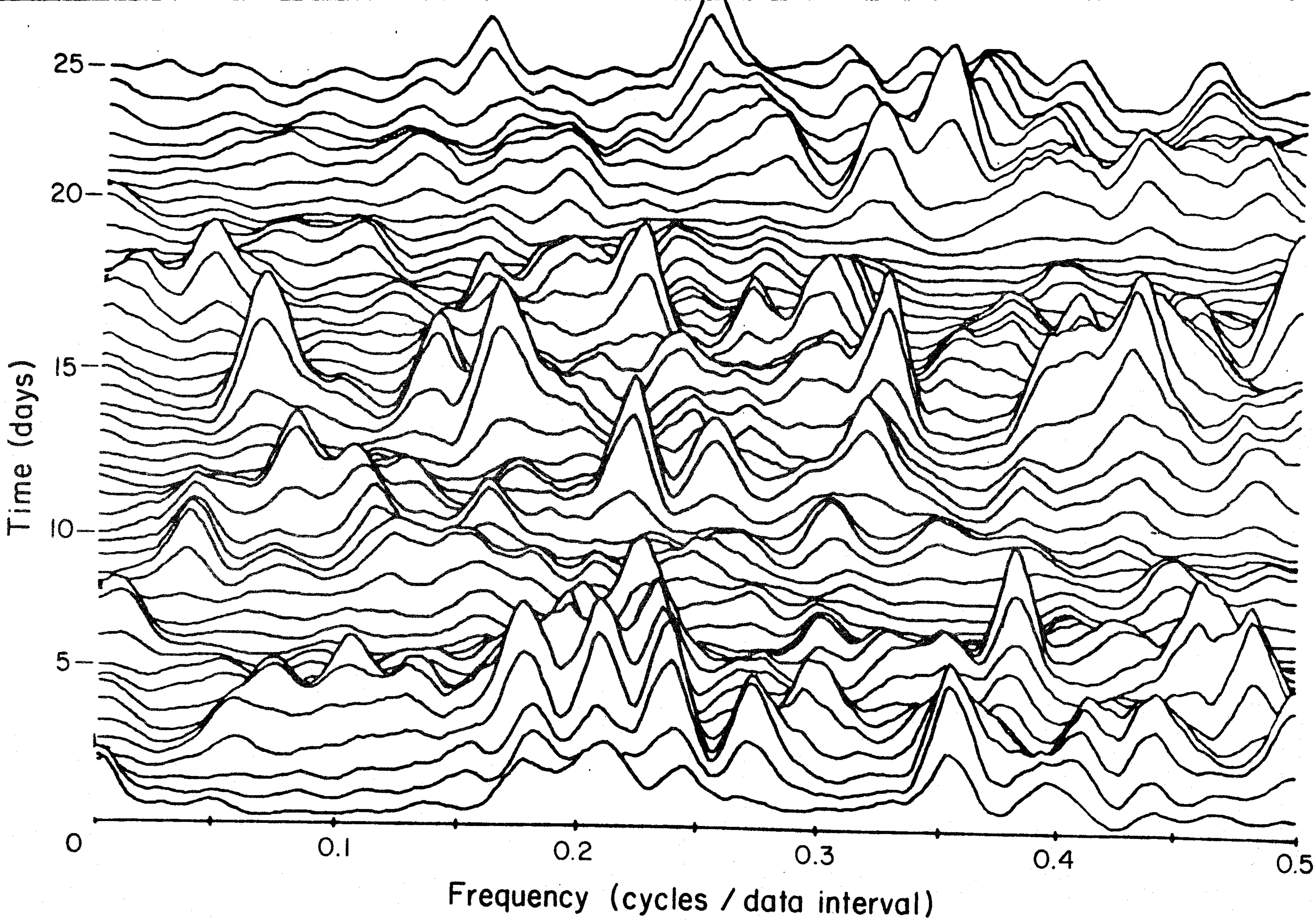

Fig. 44. Three dimensional presentation of progressive power spectra of wind speed 17 July - 11 August. Incremented 1/2 day.

Spectral analysis of the current record, 5-14 August, was performed in the same manner as the winds, Figs. 41, 42, 43. The short record allows only those events toward the high end of the mesoscale frequency range to be discerned. Because of the short record length, ten-minute interval data were used. The 12.5 hour tidal peak and the inertial period are both evident. Longer periods are lost in the first band.

Fig. 44 is a three-dimensional presentation[14] illustrating the time variation of the wind spectrum from July 17 to August 11. In this figure, frequency (cycles/data interval) increases along the horizontal axis to the right, spectral density is the topography and time increases into the picture (in perspective). The series used in forming the spectral estimates is a first-difference of the 10-min. interval wind speed series; it therefore may be considered a high-pass filtered wind speed series, a wind speed series with most of the persistence removed[15] or a wind acceleration series. Each spectral estimate is based on a 3 1/2 day segment of the series, and each segment overlaps 3 days with the preceding segment. Thus, consecutive spectral estimates correspond to times 1/2 day apart. There appear to be two intervals of relatively low energy in the fluctuating component of the wind speed; one at about one-quarter the way through the record (approximately 23 July) and the other about three-quarters of the way through (approximately 5-6 August). In the spectral plot there is also a suggestion that the spectral peaks, at least those of high frequency, increase in frequency with time. This may, however, be an illusion.

G. Comparison of Totem and Newport Winds

The OSU Marine Science Center maintains an anemometer[16] 40 m south of the South Jetty at Newport, Oregon. Hourly values of wind speed recorded at Newport during the period 16 May to 6 June were made available to us by William Gilbert. Comparison of the autocorrelation function for wind speed at Newport, Fig. 27, with that at Totem during the same period, Fig. 20, indicates that diurnal periodicity is relatively more dominant at Newport than it is at Totem. The autospectrum of wind speed at Newport, Fig. 28, is similar in character to that at Totem, Fig. 24, but the magnitude is significantly less at all frequencies. The cross-correlation function of the Totem-Newport winds, together with coherency and phase estimates, are shown in Fig. 29. Fig. 29a indicates a strong 24-hour periodicity, and the cross-correlation minimum near -70 lags suggests a periodicity of about 6 days. This figure also shows that wind speed at Totem tends to lead that at Newport by about 3 hrs. The phase lead increases with frequency in the range 0 to 0.06 cph (Fig. 29c), but as coherency drops sharply beyond this range (Fig. 29b), little can be said about phase relations at higher frequencies.

---

[14] Arand Program: *TIMSPEC, *TRISMO, *PROPLT

[15] See: Rosemary Dyer, 1971. Method for filtering meterological data. Mon. Weather Rev. 99 (5), 435-438.

[16] The anemometer (NWS Model No. F102 and F012) is mounted on a mast and is 9m above a permanent berm and 18m above mean sea level.

H. Diurnal Periodicity in Totem Winds

Spectral analysis revealed an unexpectedly large concentration of energy at the diurnal frequency in the winds at Totem. To investigate this 24-hour periodicity, series of deviations were created from 16 May to 6 June winds by subtracting from series of hourly means the mean of preceding and following 12 hr. periods. Figs. 30 a - c are plots of the 20 day averages of speed and u- and v-component deviations during each of the hours of a day, versus time of day (PDT). These figures indicate significant minima near 0900 hrs. and maxima near 1800 hrs. for deviations of the wind speed and v-component. Fig. 30e is a vector composite of the average deviations, and is similar to a progressive vector diagram.

During May there were 5 days during which meteorological conditions were quite similar: there was a steady north gradient wind associated with the Pacific High centered at 45°N, 135°W. Average deviations of wind speed during each hour of the day were computed for the 5 days and are shown in Fig. 30d. The maximum and minimum in this figure are twice as great as those of Fig. 30a. Perhaps the amplitude of the diurnal variation was especially pronounced during the selected 5 days, or there was significant variation in the times of day at which maxima and minima occurred during the total 20 day period (16 May to 6 June). An indication of the variation in amplitude of diurnal oscillations from 19 May to 4 June is shown by the complex demodulates[17] plotted in Fig. 31. It appears that significant variations of both amplitude and phase of diurnal oscillations are associated with nonstationarity of meteorological conditions.

[17] Program DEMOD

Unclassified
Security Classification

DOCUMENT CONTROL DATA - R & D

(Security classification of title, body of abstract and indexing annotation must be entered when the overall report is classified)

1. ORIGINATING ACTIVITY (Corporate author)
Oceanography
Oregon State University
Corvallis, OR 97331

2a. REPORT SECURITY CLASSIFICATION
Unclassified

2b. GROUP

3. REPORT TITLE
1970 Totem Wind and Current Data

4. DESCRIPTIVE NOTES (Type of report and inclusive dates)
Wind and current data, 1970

5. AUTHOR(S) (First name, middle initial, last name)
Members of the THEMIS Group, compiled by Noel B. Plutchak

6. REPORT DATE
May 1972

7a. TOTAL NO. OF PAGES
63

7b. NO. OF REFS
17

8a. CONTRACT OR GRANT NO.
N00014-68-A-0148

b. PROJECT NO.
NR 083--230

c.

d.

9a. ORIGINATOR'S REPORT NUMBER(S)
Data Report 52
Reference 72--13

9b. OTHER REPORT NO(S) (Any other numbers that may be assigned this report)

10. DISTRIBUTION STATEMENT
Approved for public release; distribution unlimited.

11. SUPPLEMENTARY NOTES

12. SPONSORING MILITARY ACTIVITY
Office of Naval Research
Ocean Science and Technology Division
Arlington, Virginia 22217

13. ABSTRACT

First-order analyses of wind and current time series obtained from a Totem buoy off the Oregon coast during 1970 are presented. In addition, winds at Totem are compared with winds recorded simultaneously at Newport, Oregon.

Unclassified
Security Classification

DEPARTMENT OF OCEANOGRAPHY

OSU